2007-12-14

Excess Noise in the Superconducting Transition of Tin Films

Hengsong Zhang
University of Miami, hsdx729@gmail.com

UNIVERSITY OF MIAMI

EXCESS NOISE IN THE SUPERCONDUCTING TRANSITION OF TIN FILMS

By

Hengsong Zhang

A DISSERTATION

Submitted to the Faculty
of the University of Miami
in partial fulfillment of the requirements for
the degree of Doctor of Philosophy

Coral Gables, Florida

December 2007

UNIVERSITY OF MIAMI

A dissertation submitted in partial fulfillment of
the requirements for the degree of
Doctor of Philosophy

EXCESS NOISE IN THE SUPERCONDUCTING TRANSITION OF TIN FILMS

Hengsong Zhang

Approved:

_____	_____
Dr. Fulin Zuo	Dr. Terri A. Scandura
Professor of Physics	Dean of the Graduate School
_____	_____
Dr. Stweart Barnes	Dr. Massimiliano Galeazzi
Professor of Physics	Professor of Physics

_____
Dr. Michael Wang
Professor of Electrical and Computer Engineering

ZHANG, HENGSONG (Ph.D., Physics)
Excess Noise in the Superconducting Transition of Tin Films (December 2007)

Abstract of a dissertation at the University of Miami.

Dissertation supervised by Professor Fulin Zuo.
No. of pages in text. (78)

The I-V characteristics of Tin films in the superconducting transition have been measured when ac current was applied. The experimental results suggest that the electrical response in ac is not satisfied with the I-V equation in dc. A new equation was suggested to describe the vortex motion and the vortex pair separation in the two dimensional superconducting transition with ac current, which is satisfied with our experimental results. The excess noises of Tin films in the superconducting transition have been found to depend strongly on the temperature and ac current. An empirical expression of voltage noise density in term of resistance has been used to fit the data. The peak of voltage noise density follows closely but always shifted down from dR/dT. Comparison with the dc noise measurement shows the voltage noise density with ac current is much larger than with dc current. The excess noises with ac appear earlier than the noises with dc. The difference of excess noises between ac and dc can be explained by the fluctuation of vortex pair separation process which dominates the noises generation in ac. I-V characteristics and voltage noises are measured simultaneously to reveal the nature of the excess noises. The coincidence of the excess noise and the third harmonic voltage suggests that the fluctuation of vortex pair separation process is one of the main contributions to excess noises in the two dimensional superconducting transition.

ACKNOWLEDGEMENTS

I would like to express my greatest gratitude to Dr. Fulin Zuo for his supervision and support during my graduate studies at University of Miami. Thanks to his guidance and patience, I have learned step-by-step so much first-hand experience in scientific research. I want to thank Dr. Galeazzi, Dr. Barnes, Dr. Wang, Dr. Alexandrakis, Dr. Alvarez, Dr. Ashkenazi, Dr. Cohn, Dr. Mezincescu, Dr. Nepomechie and Dr. Voss for their many helps in my research project and academic study.

I especially want to thank Mr. Marco Monti, Miss Bogorin, Miss Chen, Mrs. Chiorescu, and Mrs. Neupane for their help and collaboration during my graduate study and research in the Physics Department.

This work is supported by the Physics Department at the University of Miami and by NASA under Grant No. NNG05WC16G. These supports are gratefully acknowledged.

TABLE OF CONTENTS

Chapter 1 Introduction

1.1 Superconducting Transition

Phase transition is the transformation of a thermodynamic system from one phase to another. The typical transitions are the transitions between the solid, liquid, and gaseous states of matter. The distinguishing characteristic of a phase transition is an abrupt sudden change in one or more physical properties with a small change in a thermodynamic variable such as a temperature.

Phase transitions are divided into two broad categories according with a latent heat produced in the transition process. The first-order phase transitions are those that system either absorbs or releases a fixed amount of energy which is called latent heat during the transition process. The second-order phase transitions, which do not have associated with a latent heat, also are called continuous phase transitions. Phase transitions often take place between phases with different symmetry. Some transitions are called infinite-order phase transitions which are continuous but break no symmetries. The one example of infinite-order phase transitions is the Kosterlitz-Thouless transition in two-dimensional samples.

In 1911, zero electrical resistance of mercury was observed by H. K. Onnes who was studying the resistance of solid mercury by using the liquid helium which he had first liquefied three years before [1]. The resistance of mercury drop abruptly to zero when the temperature of sample was cooled below 4.2K. This special behavior which occurs in a wide variety of materials from metals to semiconductors was called superconducting

transition. The striking property of all superconductors is that below a critical temperature the electrical resistance of sample is zero, but at higher temperatures it is a normal metal or a semiconductor which is ordinarily not a very good conductor.

In 1933, Meissner effect which is the exclusion of the interior magnetic field was discovered by W. Meissner and R. Ochsenfeld [2]. They found that a sphere did not permit an externally applied magnetic field to penetrate into its interior when it was cooled below its critical temperature in an applied magnetic field. This effect shows the difference between a perfect conductor and a superconductor when samples are in an applied magnetic field.

So the superconductivity is characterized by two properties, zero electrical resistance and Meissner effect, when the temperature of sample is below a critical temperature. The value of critical temperature varies from material to material, ranging from less than 1K to more than 120K. Experimentally the transition from the normal state to the superconducting state has a finite transition width. There are several reasons which can explain the width of temperature over which the resistance of sample changes from its normal state value to zero. One reason is the purity of sample. The impurity of sample can broaden the transition temperature range and shifted the critical temperature to a higher temperature. The sharpness of the resistance change in the superconducting transition is an indication of the goodness or purity of the sample. Another reason of the width of temperature over the transition process is the Kosterlitz-Thouless transition which occurs in two-dimensional samples.

The third reason is an intrinsic property of the superconducting transition which is

described by the intermediate state theory. Consider a wire of radius R which is carrying a current I, the magnetic field on the surface of sample will be $2I/cR$. If the current is bigger than $I_c = H_c cR/2$ where H_c is the critical magnetic field, the magnetic field at surface will exceed the critical field, so the surface of sample will turn into the normal state. Then the current will all go through the superconducting core, which will produce a greater magnetic field on the surface of the superconducting core, so this solid superconducting core surrounded by normal state cannot be stable, the final result is that the whole sample will turn into the normal state. However in the whole normal state, the current density in the sample will be uniform across the cross section which will produce a magnetic field $H(r) = 2Ir/cR^2$, this field drops below H_c when $r \to 0$, so the superconducting core can not be wholly normal either.

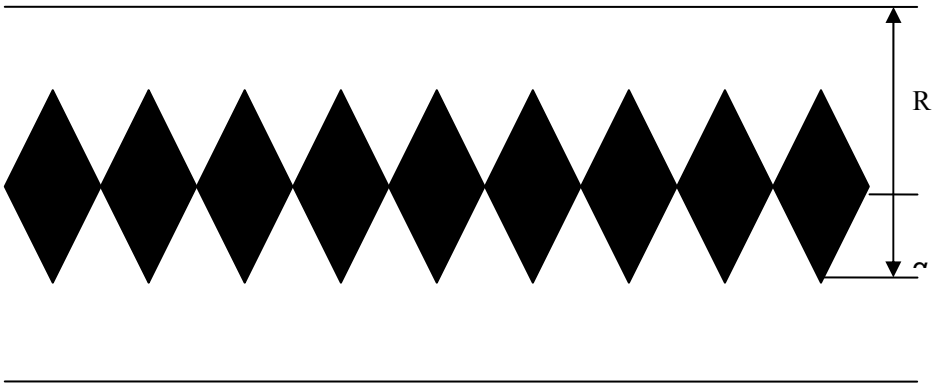

Fig 1.1 Intermediate state structure in a wire

An intermediate state was suggested by London to understand this unstable state. There is a core region of radius α which is in an intermediate state, surrounded by a normal material which also carries current. The magnetic field in the core region is satisfied with $H(r) = H_c(r \le \alpha)$, so the current density is $J(r) = \frac{cH_c}{4\pi r}(r \le \alpha)$. The

configuration in Fig 1.1, which is stable and the fractional path length of sample is r/α, was suggested by F. London to satisfy the above requirement and the longitudinal electric field is independent of the radius [3].

If the electric field produced by the electric current is E, and the resistivity of normal state is ρ, then the current density in the intermediate state is $J(r)=\frac{E\alpha}{\rho r}$, thus the radius of the intermediate can get from the requirement of the current density

$$\alpha=\frac{\rho c H_c}{4\pi E}$$

Then the current in the whole sample can be figured out

$$I=\frac{\pi R^2 E}{\rho}+\frac{c^2 H_c^2 \rho}{16\pi E}$$

From the equation above and the relationship between the critical current and the critical magnetic field, we can get

$$E=\frac{\rho I}{2\pi R^2}\left(1\pm\left(1-\left(\frac{I_c}{I}\right)^2\right)^{\frac{1}{2}}\right)$$

Compare the equation above to the relationship between the electric field E and the current I in the normal state $E=\frac{\rho I}{\pi R^2}$, we can get the resistance of sample over the transition process

$$R=\frac{R_0}{2}\left(1+\left(1-\left(\frac{I_c}{I}\right)^2\right)^{\frac{1}{2}}\right)$$

where R_0 is the resistance of sample in the normal state, $I \geq I_c$.

For the superconducting transition process according with temperature changes, the unstable pictures in the sample also exist and the intermediate model can also be used to

explain the relationship between the resistance and the temperature over the transition process. The similar equation to describe the resistance changes is given by

$$R = \frac{R_0}{2}\left(1+\left(1-\left(\frac{\Delta T}{\delta T_c}\right)^2\right)^{\frac{1}{2}}\right)$$

where $\Delta T = T_c - T$, and $\delta T_c = I\left(\frac{dI_c}{dT}\right)^{-1}$.

The resistance of sample increases continuously with the increasing temperature according to the equation above. The intermediate state region shrinks to a smaller central core with the increasing temperature until the whole sample turns into the normal state. The temperature breadth of the superconducting transition process is determined by the δT_c, which is related with the applied current. This intermediate state theory gives a good explanation of the breadth of temperature over which the resistance of sample changes from its normal state value to zero.

1.2 Vortex Motion

In 1957, Abrikosov investigated what would happen in Ginzburg-Landau theory when the penetration depth λ is larger than the coherence length ξ [4]. He indicated a negative surface energy and suggested that the sample became energetically favorable for domain walls to form between the superconducting regions and the normal regions. This kind of superconductor is called type II superconductor which is different with classic magnetic behavior of Type I superconductor in which the penetration depth λ is smaller than the coherence length ξ.

If a Type II superconductor was put into a magnetic field, the domains of normal region containing trapped flux could be formed with the low energy boundaries created between the normal core and the surrounding superconducting region. When the Ginzburg-Landau parameter $\kappa = \frac{\lambda}{\xi}$ is lager than $\frac{1}{\sqrt{2}}$, there is a continuous increase in flux penetration, which is different with the Type I superconductor in which there is a discontinuous breakdown of superconductivity in a first-order transition at critical magnetic field H_c. The applied magnetic field when the penetration starts is called the lower critical field H_{c1}, and the applied magnetic field is called the upper critical field H_{c2} when the whole sample becomes normal. Type II superconductor also have zero resistance, but only have the perfect diamagnetism when the applied magnetic field is lower than the lower critical field.

There is a mixed state, or so-called Schubnikov phase in Type II superconductors, between the superconducting state and the normal state. The magnetic flux can penetrate in quantized units by forming cylindrically symmetric domains called vortices which are in a regular array in the mixed state, the quantum of the magnetic flux is given by

$$\Phi_0 = \frac{hc}{2e}$$

where h is Plank constant, c is the speed of light, and e is the charge of electron.

Shown in Fig 1.2 is the sketch of a single vortex. There is the highest magnetic field in the core of a radius ξ which is the coherence length of sample. The core is surrounded by a superconducting region of a radius λ which is the penetration depth of sample. The shielding currents circulate around the vortex core with the current density J which decays with the distance from the core in an approximately exponential manner. Along

the axis, there is no limitation to the length of a vortex. The magnetic field lines which are perpendicular to the circulating current are continuous at the surface of sample. The individual vortices have been studied by magnetic force microscopy [5].

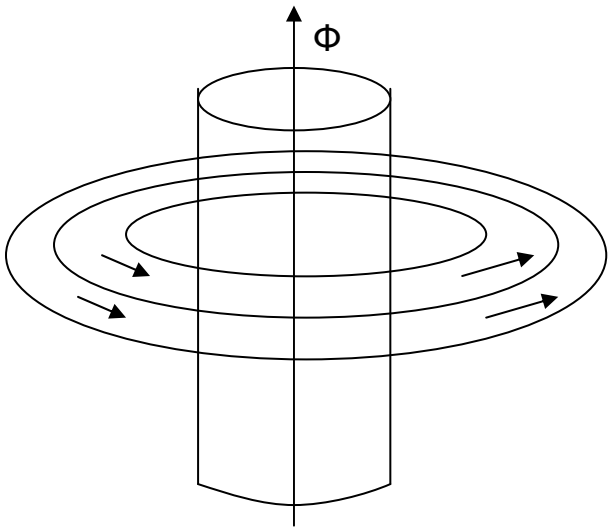

Fig 1.2 The sketch of a single vortex

To get the distance dependence of the magnetic fields and the circulating currents around the vortex core, High-kappa approximation was introduced to figure out the exact solutions of the London equations. If the Ginzburg-Landau parameter $\kappa = \frac{\lambda}{\xi}$ is much bigger than 1, or $\lambda >> \xi$, the magnetic field in the vortex can be solved from Ginzburg-Landau equation,

$$B(r) = \frac{\Phi_0}{2\pi\lambda^2} K_0(r/\lambda)$$

where Φ_0 is the quantum of the magnetic flux, and $K_0(r/\lambda)$ is a zero-order Hankel function of imaginary argument. Then we can get the current density from the magnetic field equation above,

$$J(r) = \frac{\Phi_0}{2\pi\mu_0\lambda^3} K_1(r/\lambda)$$

where $K_1(r/\lambda)$ is a first-order Hankel function of imaginary argument.

For small radial distances, $r << \lambda$, which is close to the vortex core,

$$B(r) = \frac{\Phi_0}{2\pi\lambda^2}(\ln(\tfrac{2\lambda}{r}) - \gamma)$$

$$J(r) = \frac{\Phi_0}{2\pi\mu_0\lambda^2 r}$$

where γ is the Euler constant, $\gamma = 0.577$.

For larger radial distances, $r >> \lambda$, which is far from to the vortex core,

$$B(r) = \frac{\Phi_0}{2\pi\lambda^2}(\frac{\pi\lambda}{2r})e^{-r/\lambda}$$

$$J(r) = \frac{\Phi_0}{2\pi\mu_0\lambda^3}(\frac{\pi\lambda}{2r})e^{-r/\lambda}$$

If the applied magnetic field is just slightly above the lower critical field, there are only sparsely distributed vortices through the whole sample, in which the overlap and interaction of the vortices can be negligible. With the increase of the applied magnetic field, the density of vortices increases and the distance between the vortex cores decreases. Since the shielding currents circulate around a vortex core with the same direction, the interaction between the vortices is repulsive, thus will keep the vortices as far apart as possible. The two-dimensional hexagonal vortex array in which each vortex is surrounded by a hexagonal array of other vortices is expected because of the lower free energy. In this array, the nearest-neighbor distance is

$$d = \left(\frac{2}{3}\sqrt{3}\frac{\Phi_0}{B}\right)^{1/2} = 1.075\left(\frac{\Phi_0}{B}\right)^{1/2}$$

where Φ_0 is the quantum of magnetic flux, and B is the average magnetic field inside

the superconductor. The vortex array could be demonstrated experimentally by a magnetic decoration technique coupled with electron microscopy [6-8], or by a scanning tunneling [9], or by electron holography [10].

When the average internal magnetic field is close to the lower-critical field, the lower-critical field can be given from Ginzburg-Landau theory,

$$B_{c1} = \frac{\Phi_0 \ln \kappa}{4\pi\lambda^2}$$

Thus the nearest-neighbor distance is

$$d = \left(\frac{8\pi}{\sqrt{3} \ln \kappa} \right)^{1/2} \lambda \approx \frac{3.81\lambda}{\sqrt{\ln \kappa}}$$

Because the value of $\sqrt{\ln \kappa}$ is slowly changing with κ, the distance of nearest neighbor vortices is mainly dependent on the penetration depth λ. When the average internal magnetic field is close to the lower-critical field, the equation above indicates that the vortices are separated by more than λ, i.e., only a few nearest neighbors are interacting with each other.

When the average internal magnetic field is close to the upper-critical field, the field is given by

$$B_{c2} = \frac{\Phi_0}{2\pi\xi^2}$$

and the nearest-neighbor distance is

$$d = 2\xi(\frac{\pi}{\sqrt{3}})^{1/2}$$

where ξ is the coherence length of sample, and also is the radius of the core of vortex. In this case the distance of the nearest-neighbor vortices is close to the radius of the core of

vortex, which means the vortices are almost overlapping.

When the average internal magnetic field is between the lower-critical field and the upper-critical field, not only the nearest-neighbor vortices, but also many vortices far from the selected vortex are within the interaction range of the selected vortex. Thus the group activity needs to be checked and more detailed calculated are required, but the details of the core of vortex still can be neglected.

For a single vortex, there will be the mutual-repulsion Lorentz force from the other vortices and from the applied transport current, which will lead to the vortex motion. If there is an isolated vortex Φ_0 in a region of constant current density J, the vortex will experience a Lorentz force

$$f_L = J \times \Phi_0$$

The vortex also is retarded by a viscous damping force

$$f_v = \beta v$$

and experience a Magnus force which is exerted on a spinning object through a fluid medium, i.e., there is a force exerted on the moving vortex in a direction at right angles to its speed. The force is given by

$$f_M = \alpha n_s e(v \times \Phi_0)$$

where n_s is the density of superconducting electrons. Because the viscous damping force and the Magnus force are dependent on the velocity of vortex, the Lorentz force would be balanced by the two velocity-dependent forces when the velocity is increased to reach a steady-state motion. The equation of the steady-state motion will be

$$J \times \Phi_0 - \alpha n_s e(v \times \Phi_0) - \beta v = 0$$

According to the equation above, the vortex velocity at the steady-state motion can be given by

$$v = \frac{J\Phi_0}{\left[\beta^2 + (\alpha n_s e\Phi_0)^2\right]^{1/2}}$$

$$\tan\theta = \alpha n_s e\Phi_0 / \beta$$

where θ is the angle between the vortex speed and the Lorentz force. If the Magnus force is small and can be neglected, the vortex velocity can be simplified by

$$v = \frac{J\Phi_0}{\beta}$$

The vortex velocity at the steady-state motion increases with the increasing applied current. But the bigger the viscous coefficient and the bigger the Magus force coefficient, the slower the vortex velocity at the steady-state motion.

The equation of steady-state motion above is only derived for the motion of individual vortices, i.e., the equation can be applied only when the average internal magnetic field is close to the lower-critical field. When the average internal magnetic field is close enough to the upper-critical field, there are great overlaps of vortices in sample, which means an array of vortices should be considered a continuum of magnetic flux. The continuum of magnetic flux acts like a highly viscous fluid which moves in large groups under the action of perturbing forces. The density of the condensed vortex phases is not fixed, instead of over a range of densities from $\rho_{\min}$ to $\rho_{\max}$, the relationship of these two limitations can be given by

$$\frac{\rho_{\max}}{\rho_{\min}} \approx \left(\frac{\lambda}{\xi}\right)^2$$

According to the steady-state motion equation above, in the presence of a transport

current in sample, the vortices will move from one side to the other at velocity υ, thus will induce a longitudinal resistive voltage across the sample. The voltage across the width W will be the sum of a large number of pulses which will display a sort of shot noise spectrum. The frequency of shot noise is given by

$$f \approx \frac{1}{\tau} = \frac{\upsilon}{W}$$

The shot noise nature also holds when the vortices move in bundles. The noise spectrum was measured by van Ooijen and van Gurp which is satisfied with the theoretical calculation [11].

The motion of vortex from one side to the other means a magnetic field moves across the sample at a constant speed, thus the vortex motion will produce an electric field which is perpendicular to both the speed and the magnetic field. The electric field produced by the vortex motion is the same direction as the applied current. This voltage drop along the direction of the applied current gives a mechanism of the resistance of type II superconducting sample in the transition process.

In a real sample, there is always a pinning force which sometimes can hold the core of a vortex in a fixed location. The pinning force is a short-range force which is produced by the in-homogeneity of sample, such as a point defect, or a columnar defect, or a screw dislocation, or a grain boundary, and so on. Until the applied current is big enough and the Lorentz force is capable of exceeding the pinning force, the vortex will be held in place and there is no longitudinal resistive voltage produced.

Flux motion is strongly dependent on the vortex pinning which is present in all real samples. When the pinning force is large enough and dominates, sometimes thermally

activated fluctuation can lead to a very slow vortex motion. This slow vortex motion is called flux creep and lead to a small longitudinal resistive voltage [12]. When the applied current is big enough and the Lorentz force dominates, the vortex will move fast which is called flux flow [13, 14]. Some new phases, including Bose glass [15, 16], vortex glass [17, 18], are introduced to explain the flux motion subject to the action of thermal fluctuation or correlated pinning force. These new phases can be strongly influenced by the type of artificial pinning centers.

1.3 Kosterlitz-Thoulesss Transition

We have introduced the vortex motion which is induced by the external magnetic field in last section. There are still other vortices produced by the thermal perturbation at low temperatures. Thermal fluctuation can create positively and negatively oriented vortices. These vortex and anti-vortex pairs sometimes are called intrinsic vortices. Normally, the number of intrinsic vortices in sample is much more than the vortices induced by the external field. The flux and the shielding currents of an anti-vortex which circulate around the vortex core flow in a direction which is opposite to that of the vortex, so a vortex and an anti-vortex will attract each other.

For a two dimensional sample, if the temperature is lower than a critical temperature T_c, there will be a lager number of intrinsic vortices in samples even in the absence of an external magnetic field. The vortices will flow in the sample and produce the resistance which we discussed in last section. If a pair of vortices which have the opposite flux

direction and the opposite circulation shield current are close enough where the distance between the vortex and the anti-vortex is less than the transverse penetration depth, the interaction energy of vortex and anti-vortex pair is logarithmic in the separation. Theory predicts that the vortex and the anti-vortex will form bound pairs at this temperature, which will lead to the topological long-range order.

When the temperature is below T_c, the electrical response of thin films will be dominated by the presence of bound pairs of thermally excited vortices of opposite circulation. When the temperature is above T_c, because the order-parameter correlation function decays exponentially, the electrical response will be dominated by a lager number of free vortices due to the thermal perturbation. Thus there will be a vortex anti-vortex unbinding transition at temperature T_c which was first discussed by Kosterlitz & Thouless [19] and by Berezinskii [20]. This topological phase transition was called Kosterlitz-Thouless transition and has been experimentally verified in superconductors [21-23]. The critical temperature of K-T transition is a little lower than the usual superconducting critical temperature.

One of the methods to figure out the critical temperature of K-T transition is to measure the current-voltage characteristics of sample. When the temperature is below T_c, there are a lot of bound vortex pairs in sample. When a current is applied in sample, the bound vortex pairs will be separated into the free vortices by the current. The number of free vortices will increase with the increasing current, so the resistance produced by the free vortices motion will increase with the increasing current too. The relationship between the voltage across the sample and the applied current is not linear any more.

Theory predicts a I-V dependence for T< T_c of the from [24]

$$V = 2R_n I_0 (a(T) - 3)(I / I_0)^{a(T)}$$

Where a(T) is a power-law exponent, I_0 is the critical current of sample. So the critical temperature can be determined from nonlinear I-V characteristic for T< T_c and a pronounced crossover from nonlinear towards linear dependence for T>T_c. Shown in Fig 1.3 is a typical log-log plot of the I-V characteristics of K-T transition [25] and the critical temperature of K-T transition can be determined by the highest temperature at which no deviation from power-law behavior at low currents.

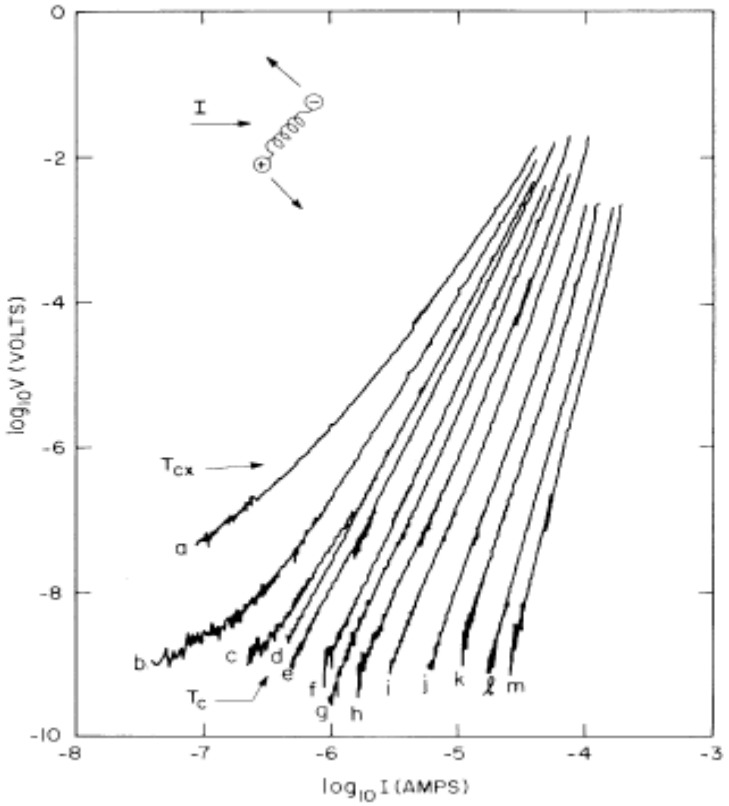

Fig 1.3 Plot on logarithmic axes of the I-V characteristic

When the temperature of sample is above the critical temperature, there are a large number of free vortices produced by thermal perturbation in sample which gives the linear I-V characteristic at small currents. The resistance from this linear I-V

characteristic can be measured in term of the temperature. Theory predicts the temperature dependence near T_c of the form [24]

$$R = \alpha R_n \exp\{\frac{-2\beta}{(T-T_c)^{1/2}}\}$$

Where α and β are constants. Shown in Fig 1.4 is the plot for $T>T_c$ of the logarithmic axes of the resistance as a function of $(T-T_c)^{-1/2}$ where T_c=1.903K [25]. The data in Fig 1.4 were taken at low enough currents to assure the nonlinear pair breaking was not occurring and is satisfied with the theoretical equation.

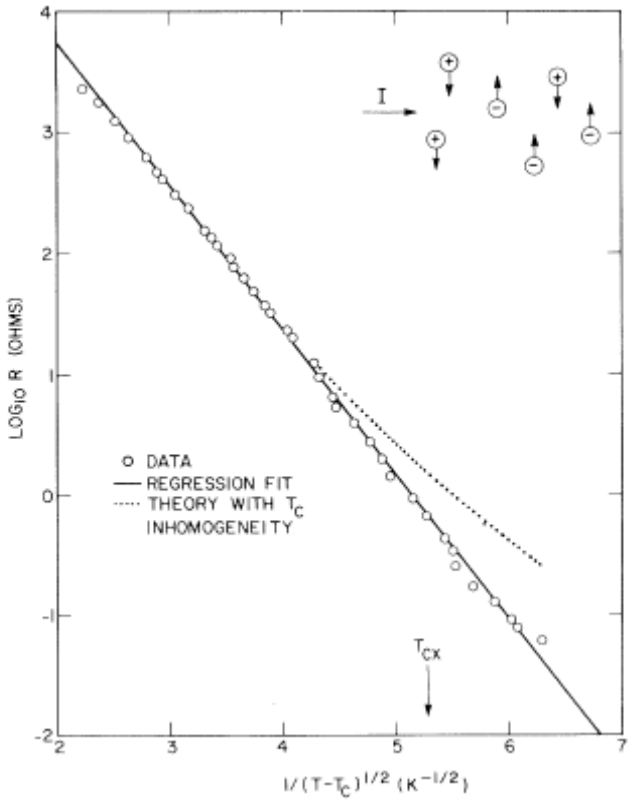

Fig 1.4 Plot for $T>T_c$ of the logarithm of the resistance as a function of $(T-T_c)^{-1/2}$

1.4 Excess Noise in TES Microcalorimeters

The fast detector system is required in x-ray astrophysics missions, which is capable

of imaging spectroscopy with the highest possible energy resolution and quantum efficiency, and is combined with the ability to be used on extended sources without spectral degradation. X-ray microcalorimeters based on transition edge sensor offer the best performance which have resolution superior to the silicon or NTD Germanium-based [26] energy dispersed spectroscopy, and have the fast response time due to negative electrothermal feedback [27].

A transition edge sensor is typically a superconducting thin film which is working in the phase transition between the normal state and the superconducting state. The energy of the incident x-ray was absorbed and converted into heat by an absorber, and a transition edge sensor was used to detect the temperature variations of the absorber. There is a weak link between the detector and a heat sink to control the working temperature [28]. The resistance of sensor is very sensitive to the temperature variations which can be characterized by the sensitivity

$$\alpha = \frac{T}{R}\frac{dR}{dT}$$

where T and R are the temperature and the resistance of the sensor respectively. The most commonly used transition edge sensor are AL-Ag, Mo-Au, Mo-Cu, Ti-Au, and Ir-Au bi-layers or W thin films with the transition temperature typically in the 100mK range.

Theoretically the energy resolution is determined by the sensitivity of sensor, there are also two fundamental contributions which can affect the energy resolution of sensor [29]. The first is the Johnson noise of sensor which is a voltage noise across a finite resistor and produced by the thermal perturbation. The voltage spectral density of Johnson noise can be given by $\sqrt{4k_B TR}$ where k_B is the Boltzman constant. The

second is the thermal fluctuation noise between the sensor and the heat sink through a weak link, which is produced by the random passage of phonons through a finite thermal conductance G. The thermal fluctuation noise consists of a white noise spectrum with a power spectral density proportional to $\sqrt{4k_B T_0^2 G}$. The electronic noise from the readout electronics can usually be neglected with suitable choice of amplifiers.

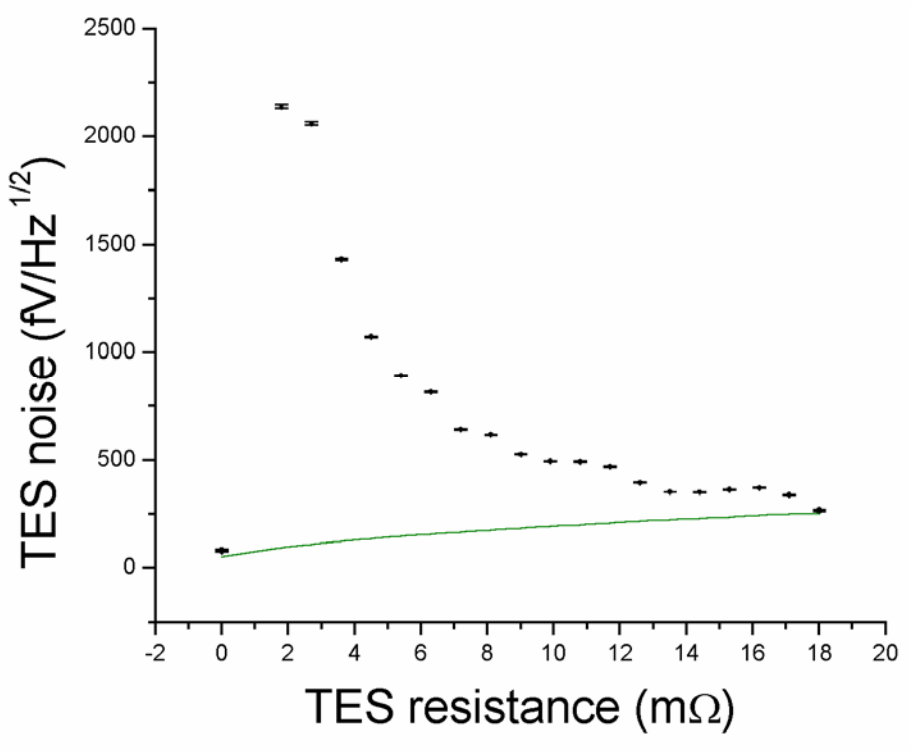

Fig 1.5 The excess noise versus detector resistance

The actual noises of transition edge sensors measured by several groups are much larger than the calculated results which include the Johnson noise and the thermal fluctuation noise. Shown in Fig 1.5 is the resistance dependence of the voltage noise density of detector [30]. The data is taken at high frequencies so that the thermal fluctuation noise can be neglected. The noise of detector increases drastically with the decreasing resistance and is much bigger than the Johnson noise which corresponds to the line in Fig 1.5. The excess noises dramatically decrease the sensitivity of transition edge

sensors.

To understand the source of excess noises so that we can reduce the excess noises of sensors and optimize the performance of microcalorimeters, concerted effects are being put together to study how excess noises are effected by various parameters, such as the composition of transition edge sensor materials, the geometry of the detector from square film to trapezoid or Corbino disk, edge treatment, resistance and bias voltage. The results up to date are inconclusive and sometimes controversial among various research groups. [31-33]

Since the excess noises depend on various parameters, it is believed that the excess noises may be dominated by fundamental physics in the transition edge sensor. This includes the effect of flux motion due to self-field and external-field, and the fluctuation of the superconducting order parameter in the transition region. So the research on the flux motion and superconducting fluctuation in thin films will help us to understand the source of excess noises better.

The flux can be generated by the external applied field or due to the self-field of the transport current. The form of flux in thin films is complicated and dependent on the thickness of film and the magnetic penetration depth. When a current is applied in a thin film, flux lines or domains will move transverse to the applied current due to the Lorentz force. Shown in Fig 1.6 is the schematic of the magnetic behavior of superconducting strip carrying transport current [34].

For a small current, the magnetic field associated with the current is completely expelled from the specimen due to Meissner effect, and only exists on a surface layer with

the thickness of λ. Thus the current flows mostly along the edges of the strip. With the increase of current or temperature, the magnetic field of the current will increase to reach a value of the order of the critical field at the sample edges, a normal region will be created locally at the edges. Due to the resistance of this normal region, the transport current will try to avoid this region and flow along the surface of the superconducting region. Because the magnetic filed is enhanced at the inside of this current loop, the process above will repeat and the normal region will grow abruptly until it reaches the center of the strip. When the normal region reaches the center, the current can not find a path in superconducting region any more, then the magnetic field will exist in the whole normal region thus will be less than the critical field, so the whole normal region will turn into the superconducting state again. This is analogous to the kink instability in magneto-hydrodynamics.

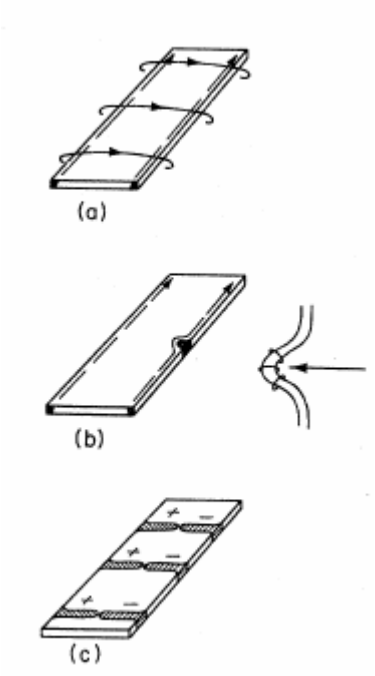

Fig.1.6 Magnetic structure due to transport current: a) Meissner effect; b) nucleation of a domain at the edge; c) magnetic structure at high current density.

For a big current, the current will induce a magnetic structure which consists of

many channels of the normal phase. The channel of normal state will grow from both edges to the center of the strip. Because the magnetic fields in these channels have opposite signs at the two sides of the strip, the vortices created at the edges will be pushed by Lorentz force toward the center of the strip, and be annihilated by the vortices of opposite sign from the other side of the strip.

Either for a small current or for a big current, the configuration in thin films is magnetically unstable. Thus the fluctuations in time of the number of normal domains or normal channels will produce the voltage noises in thin films. The current induced magnetic structure and its dynamics have been studied and verified in classical superconductors. [35-37]

Another possible source of the excess noise is the fluctuation of the number of superconducting pairs or superconducting order parameter near the transition temperature. The number of superconducting pairs n_s in the absence of magnetic field can be calculated by Ginzburg-Landau theory,

$$n_s = |\psi_0|^2 \propto (1 - \frac{T}{T_c})$$

then we can figure out the temperature dependence of various parameters. Actually, there is always thermal fluctuation at a finite temperature, which will lead the fluctuation in the order parameter itself and consequently in the number of superconducting pairs. The fluctuation of order parameter $\delta\psi$ will be give by

$$\frac{(\delta\psi)^2}{\psi^2} \propto \frac{1}{(1 - \frac{T}{T_c})^2}$$

Normally the relative change in the number of superconducting pairs is very small, but if

T is very close to the critical temperature T_C, the fluctuation will be big which can be figured out by including the higher order terms in the expansion to eliminate the divergence. The fluctuation effect is most pronounced near T_C for the temperature both above and below the transition.

Some n_s-sensitive techniques can be used to measure the effects of superconducting fluctuation. Most often technique is either to measure the magnetic susceptibility or to measure the excess conductivity above T_C. [38,39]

Chapter 2 Current-Voltage Characteristics

2.1 Experimental Setup

Our samples are thin granular tin films which were deposited on glass substrates by thermal evaporation process. The films were deposited in vacuum ($5x10^{-5} torr$) with the rate of 1-3Å/sec. The structure of Tin film is shown in Figure 2.1. A typical film has a dimension of 0.4mm x 10mm and the thickness varying from 500-1500Å. Silver wires were attached to the four ends of samples by using conducting silver paint to perform a four-point voltage measurement. The resistance of sample at room temperature varies from 20-90 ohm, and the sheet resistance is about 1-4 ohm/□ at room temperature. The resistance of sample will decrease to about 2-9 ohm at temperatures close to the critical temperature. Typical temperature of superconducting transition is about 3.80K. The critical temperature has a small variation which depends on the deposition rate and the thickness of sample. The temperature width of transition is about 20-40mK.

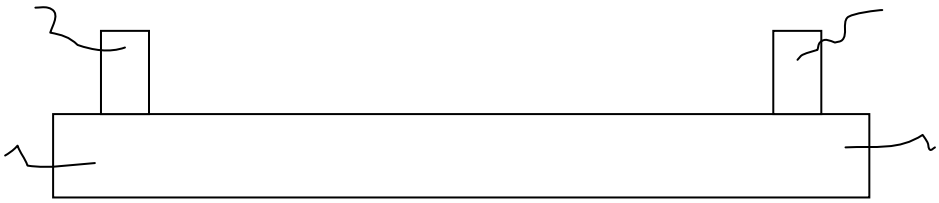

Fig 2.1 The structure of Tin film

The sample is immersed in the liquid Helium bath for thermal stability. For constant temperature measurements the temperature is controlled by pumping on the bath. The current-voltage characteristics of sample and the relationship between the voltage noise

and the applied current at fixed temperatures were measured during the transition process. The temperature dependence of the current-voltage characteristic and the temperature dependence of the voltage noise were measured when the bath is slowly pumping down or slowly warming up. Typical cooling down or warming up time through transition is about 1-3 hours, thus the typical temperature drifting rate is 10-30μK/sec.

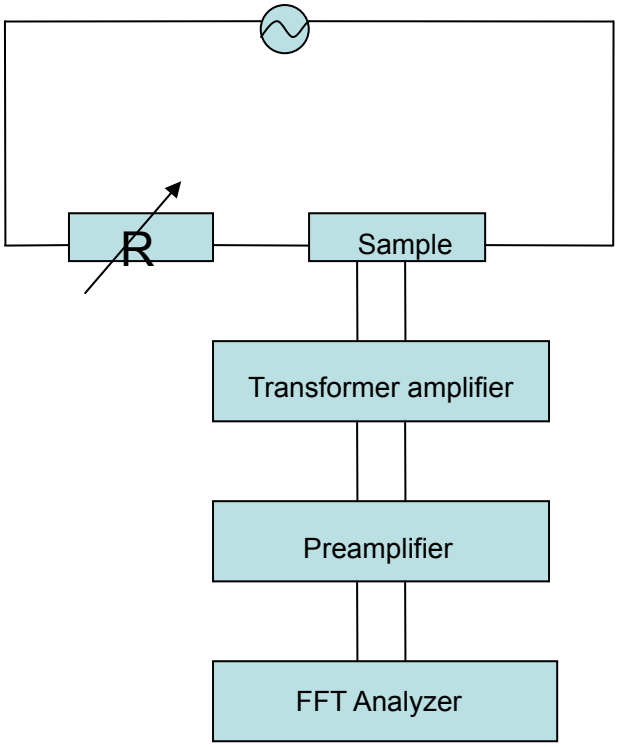

Fig 2.2 Schematic of the experimental setup

The basic schematic of the noise measurement setup is shown in Fig 2.2. Both ac and dc excitation currents have been used during the current-voltage characteristic measurement and the noise measurement. For the current-voltage characteristic measurement, Keithley 182 sensitive digital voltmeter was used to record the voltage of sample when the direct current was applied. When the applied current is a sine-wave alternating current which the frequency is typically at 16 Hz, SR760 spectrum analyzer

was used to record the fundamental voltage and the harmonic voltages at the same time. For the noise measurement, three stage amplifications were used to amplify and filter the signal. The noise signals were first fed into SR554 low noise transformer preamplifier and followed by two stages of SR560 low noise preamplifiers. The noises were measured typically at 1 KHz and the total amplification is 10^5. Sometimes SR860 Lock-in amplifier was used to record the fundamental voltage in the noise measurement to establish the relationship between the current-voltage characteristics of sample and the excess noises in the transition process. The applied alternating current is limited below 1000μA to avoid magnetization of the transformer amplifier.

2.2 Current-Voltage Characteristics

Current-voltage measurement is one of the most used methods to study the flux motion, vortex pinning mechanism and dimensional crossover in superconducting transition. In a two-dimensional superconductor, Kosterlitz-Thouless transition plays an important role in the transition process. When the temperature was at the lower part of the transition temperature width, the vortex pairs were separated by the applied current so that the relationship between the voltage across the sample and the applied current would not be linear. When the temperature reaches the critical temperature of K-T transition, the linear term of current-voltage characteristic appears, demonstrating that free vortices are now produced in sample by the thermal perturbation. The log-log plot of the current-voltage curves of Tin films is shown in Fig 2.3 and displays a typical

current-voltage characteristic of K-T transition.

When the temperature is at the lower part of the transition temperature width, the current-voltage characteristic in the two dimensional superconducting transition is given by

$$V = KI^{\alpha} \qquad (2.1)$$

where K and α are real numbers which depend on the temperature. During the transition process over which a superconducting sample turns into the normal state with the increasing temperature, the power index α decrease continuously from a big number to one (linear relationship in normal state).

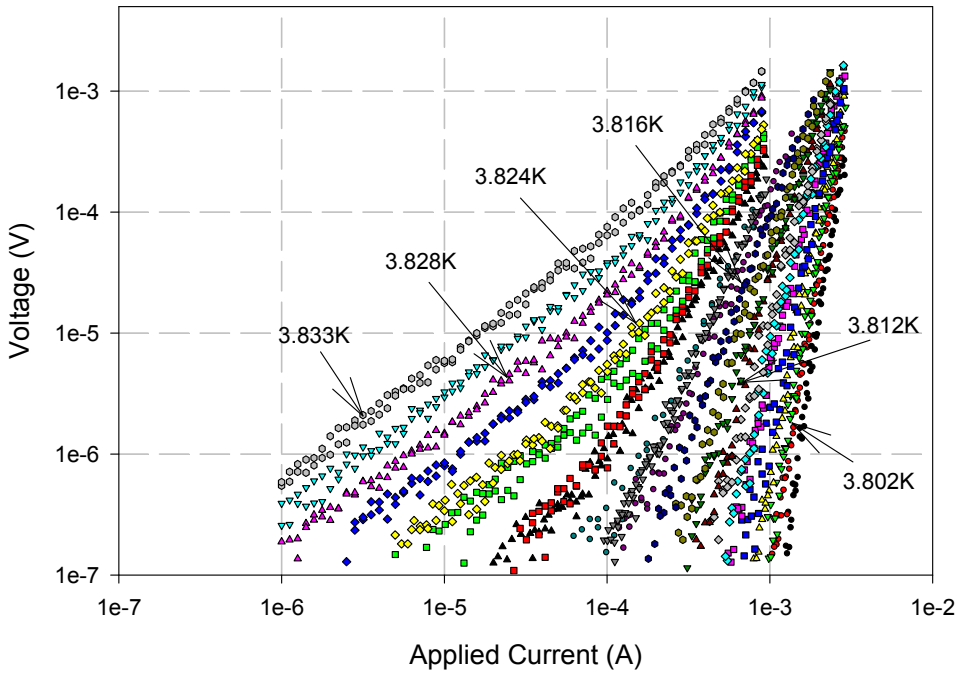

Fig 2.3 Log-log plot of the I-V curves (Sample 17)

Normally the applied current is a direct current when we talk about the voltage-current characteristics of samples. An interesting question is, if we use an alternating current as the excitation current, is the relationship between the voltage across the sample and the applied current still satisfied with the equation above? If the answer is

no, what will be the relationship between the voltage and the alternating applied current?

According to equation (2.1), if a sine-wave alternating current was used as the excitation current, the equation will be

$$V = K(\sin(\omega t))^{\alpha} I^{\alpha}$$

Normally this equation is complicated to deal with, but when the power index α is a natural number, it can be easily expanded by using trigonometric identities:

$$\alpha = 2 \qquad V = (\frac{1}{2} - \frac{1}{2}\cos(2\omega t))I^2$$

$$\alpha = 3 \qquad V = (\frac{3}{4}\sin(\omega t) - \frac{1}{4}\sin(3\omega t))I^3$$

$$\alpha = 4 \qquad V = (\frac{3}{8} - \frac{4}{8}\cos(2\omega t) + \frac{1}{8}\cos(4\omega t))I^4$$

$$\alpha = 5 \qquad V = (\frac{10}{16}\sin(\omega t) - \frac{5}{16}\sin(3\omega t) + \frac{1}{16}\sin(5\omega t))I^5$$

$$\alpha = 6 \qquad V = (\frac{10}{32} - \frac{15}{32}\cos(2\omega t) + \frac{6}{32}\cos(4\omega t) - \frac{1}{32}\cos(6\omega t))I^6$$

$$\alpha = 7 \qquad V = (\frac{35}{64}\sin(\omega t) - \frac{21}{64}\sin(3\omega t) + \frac{7}{64}\sin(5\omega t) - \frac{1}{64}\sin(7\omega t))I^7$$

…… (2.2)

According to the expanded equations above, when the power index is an even number, there is no term in expanded equations which has the same frequency as the frequency of applied current (i.e. fundamental frequency). So if equation (2.1) is still satisfied with the alternating applied current, when the temperature dependence of the fundamental voltage in the superconducting transition are measured, there is supposed to be several zero voltages where the power indexes of the current-voltage characteristic are even numbers, the voltage dips with the increasing temperature are expected in the transition process. Fig 2.4 shows the temperature dependence of the fundamental voltage in the superconducting transition. The applied current is a 200μA sine-wave alternating

current. The logarithmic scale is used on Y dimension (voltage dimension) to expand the small voltage in the lower temperature. There is no voltage dip in the plot of transition process in Fig 2.4, which suggests that the equation (2.1) may be not suitable for the alternating applied current.

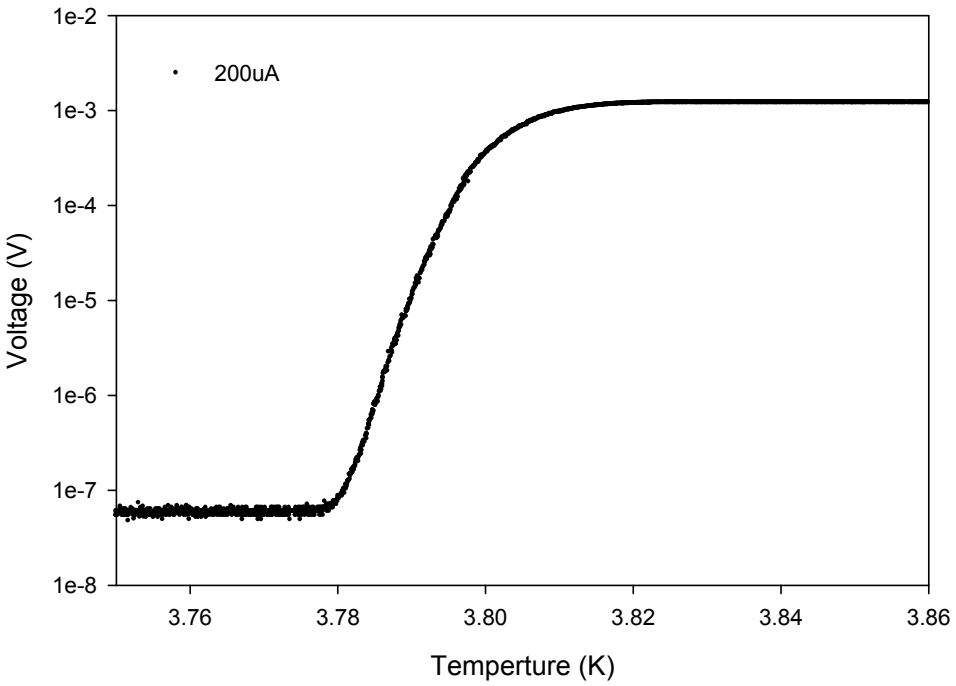

Fig 2.4 The temperature dependence of the fundamental voltage (Sample 4)

2.3 Even Power Indexes

In our experiment the current-voltage characteristics of Tin films were studied carefully. Shown in Fig 2.5 is the current-voltage relationship with the direct applied current at 3.767K. The linear relationship between logarithmic voltage and logarithmic current indicates that the current-voltage characteristic of Tin film is satisfied with equation (2.1). The slope of regression line in Fig 2.5 is close to 4, which means the power index in equation (2.1) is about four.

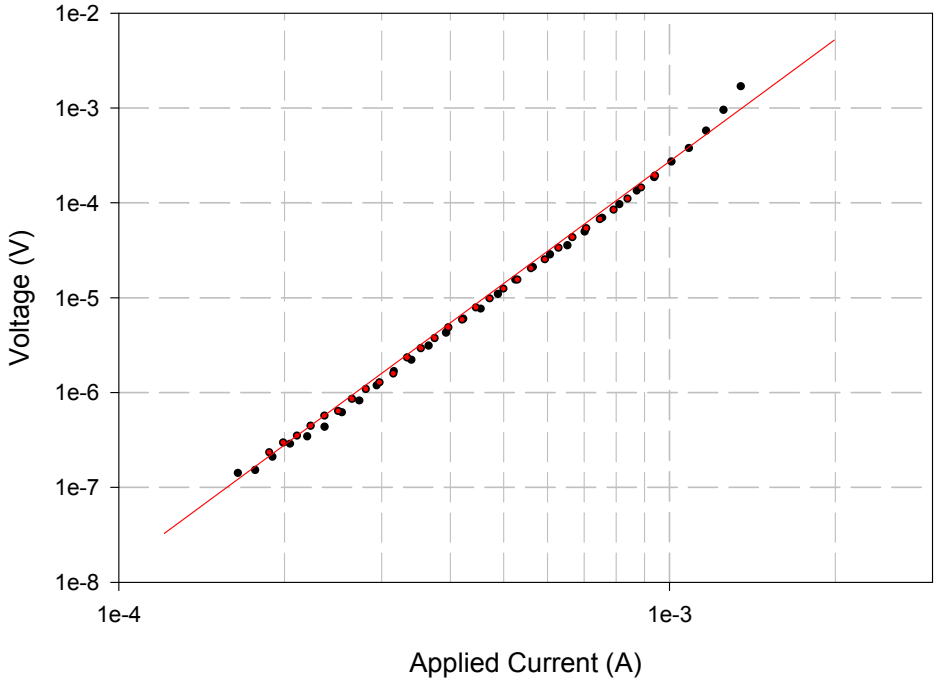

Fig 2.5 I-V characterisc of sample at 3.767K (Sample 4)

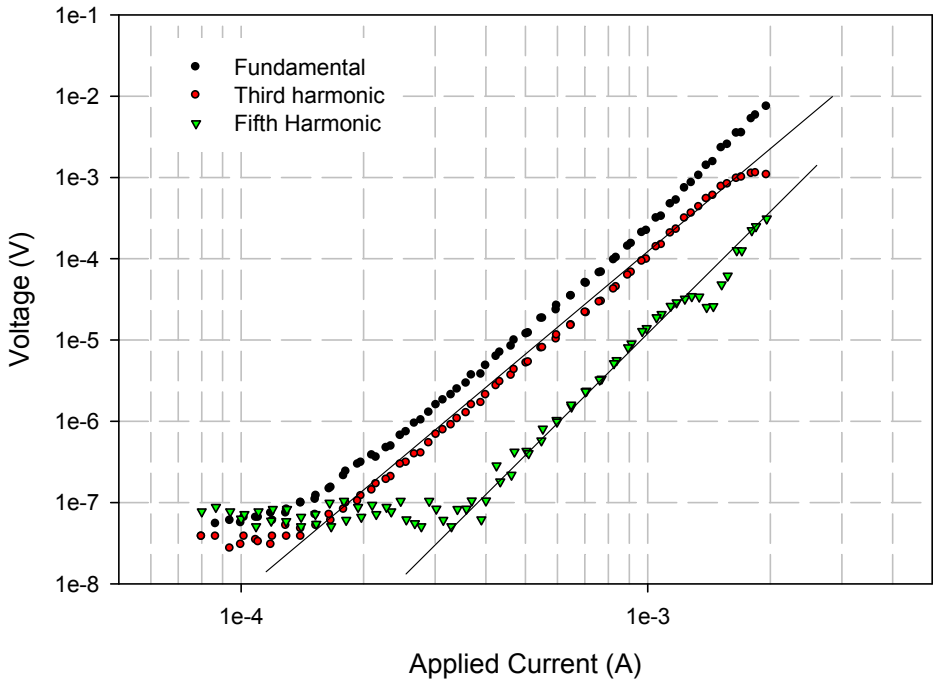

Fig 2.6 I-V characteriscs of sample at 3.767K (Sample 4)

According to the trigonometric expanded equation (2.2),

$$\alpha = 4 \qquad V = (\frac{3}{8} - \frac{4}{8}\cos(2\omega t) + \frac{1}{8}\cos(4\omega t))I^4$$

if equation (2.1) is still satisfied with the alternating applied current, the second harmonic

voltage and the fourth harmonic voltage across the sample are expected at 3.767K, instead of the fundamental voltage, the third harmonic voltage, and the fifth harmonic voltage. However the SR760 spectrum analyzer showed that neither the second harmonic voltage nor the fourth harmonic voltage was recorded in the sensitive range. Actually, the fundamental voltage, the third harmonic voltage, and the fifth harmonic voltage were recorded in the spectrum analyzer at the same time. Fig 2.6 shows the overlay of the log-log plots of the fundamental voltage, the third harmonic voltage, the fifth harmonic voltage versus the applied current.

The power indexes can be easily obtained in the log-log plot. The slope of fundamental voltage versus current is about 4, which is the same as the slope of current-voltage in Fig 2.5 where the applied current is a direct current. The slope of third harmonic voltage versus applied current is also about 4. However the slope of fifth harmonic voltage versus applied current is about 5, which is different with the slopes of the fundamental voltage plot and the third harmonic voltage plot.

Shown in Fig 2.7 are the current-voltage characteristics of sample at 3.759K with the direct applied current. Equation (2.1) is still satisfied at this temperature according to the plot in Fig 2.7. The slope of the logarithmic voltage versus logarithmic current indicates that the power index in equation (2.1) at this temperature is about 6.

Same as the discussion above, according to the equation (2.2),

$$\alpha = 6 \qquad V = (\frac{10}{32} - \frac{15}{32}\cos(2\omega t) + \frac{6}{32}\cos(4\omega t) - \frac{1}{32}\cos(6\omega t))I^6$$

the second harmonic voltage, the fourth harmonic voltage and the sixth harmonic voltage are supposed to be recorded in the SR760 spectrum analyzer if a sine-wave alternating

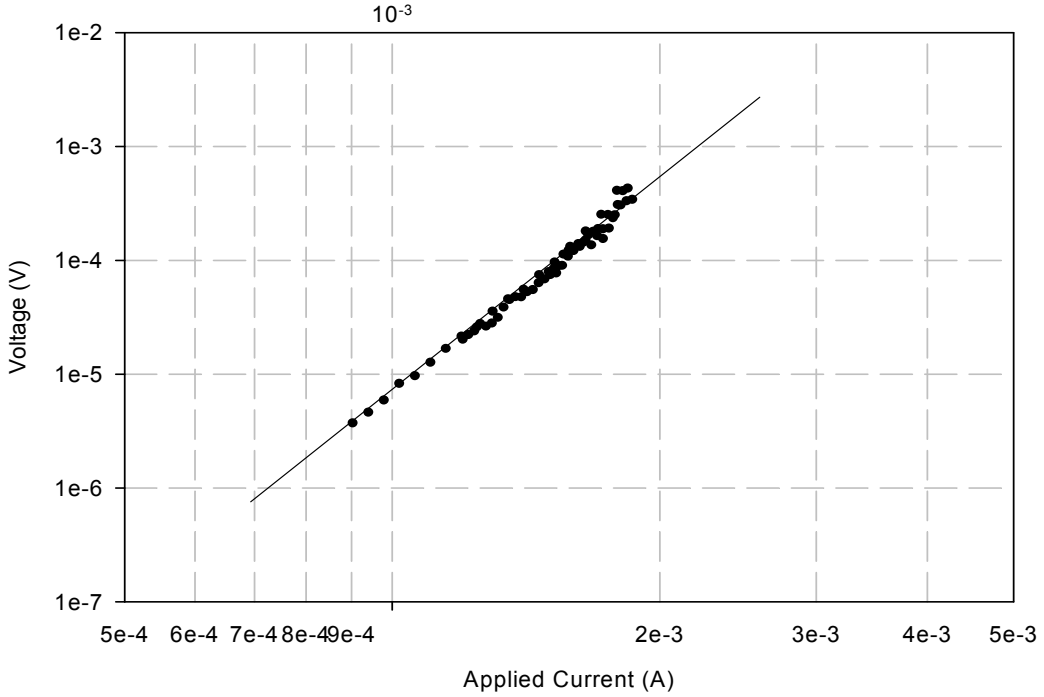

Fig 2.7 I-V characterisc of sample at 3.759K (Sample 4)

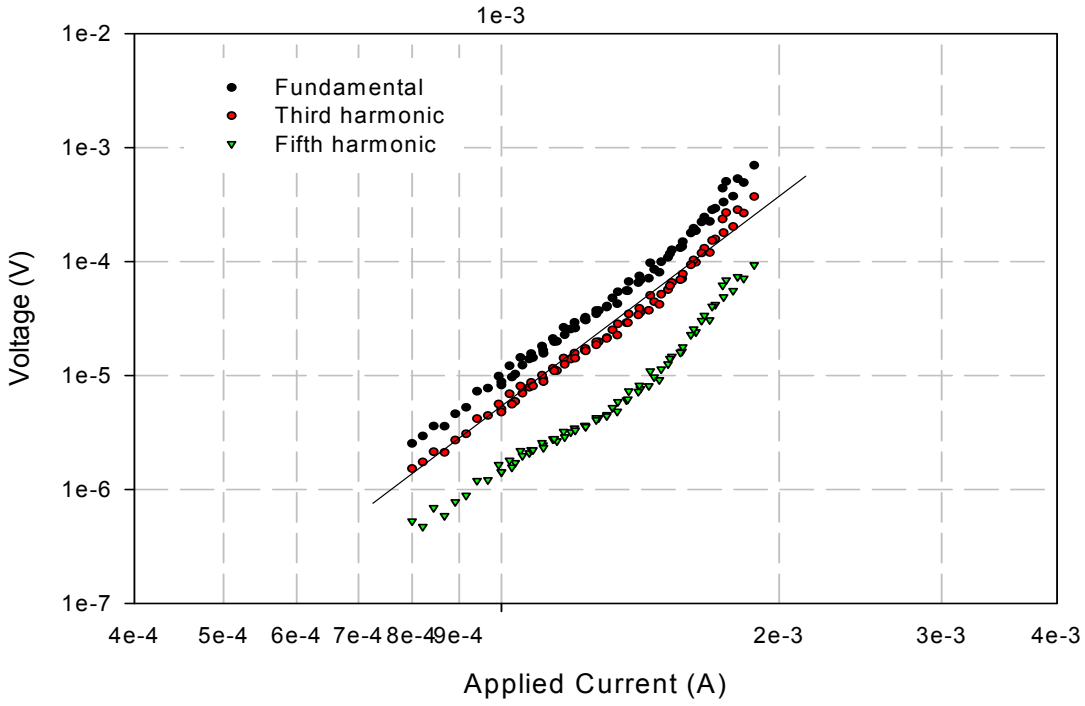

Fig 2.8 I-V characteriscs of sample at 3.759K (Sample 4)

current was applied at this temperature. However the experimental results show that only the fundamental voltage, the third harmonic voltage and the fifth harmonic voltage were recorded in the spectrum analyzer. Shown in Fig 2.8 is the overlay of log-log plots of

current-voltage at 3.759K for the alternating applied current. Different with the plots in Fig 2.6, all three current-voltage curves have the same slope 6 which is the same as the slope of the plot of direct current.

The experimental data suggest that equation (2.1) is not satisfied with the alternating applied current. Equation (2.1) describes the process of vortex pair unbinding. For a direct applied current, the number of separated vortex pairs is decided by the temperature and the amplitude of excitation current, thus the voltage across the sample, which is related with the number of free vortices, is constant at a fixed temperature and a fixed current. However for an alternating applied current, the number of separated vortex pairs fluctuates with the alternating applied current, which is totally different with the case of direct applied current.

2.4 Current-Voltage Equation

The voltage of a sample in the superconducting transition is decided by the applied current and the resistance which is linear with the number of free vortices. The number of free vortices in the sample also depends on the applied current, so the number of free vortices is a function of current, i.e. $N = N(I)$. Because the number of free vortices is independent on the direction of applied current, $N(I)$ is an even function of current which can be expanded in a small current by

$$N(I) = N_0 + \frac{1}{2!}\frac{\partial^2 N}{\partial I^2} I^2 + \frac{1}{4!}\frac{\partial^4 N}{\partial I^4} I^4 + \frac{1}{6!}\frac{\partial^6 N}{\partial I^6} I^6 + \cdots \qquad (2.3)$$

So the voltage of sample will be given by

$$V \propto IN = IN_0 + \frac{1}{2!}\frac{\partial^2 N}{\partial I^2} I^3 + \frac{1}{4!}\frac{\partial^4 N}{\partial I^4} I^5 + \frac{1}{6!}\frac{\partial^6 N}{\partial I^6} I^7 + \cdots$$

That is to say, for a small applied current, the current-voltage characteristic can be expressed by

$$V = AI + BI^3 + CI^5 + DI^7 + \cdots \qquad (2.4)$$

where coefficient A, B, C and D depend on the temperature. The first term AI is attributed to the free vortex motion and coefficient A should be linear with the resistance of sample. Because the interaction of two vortices is supposed to be linear with $(I\phi)^2$, the second term BI^3 should be the contribution of the separation of vortex pairs, and the third term CI^5 can be considered the contribution of vortex pair-pairs. There are still higher power terms in equation (2.4), which are attributed to the other vortex groups, but here we only discuss the first four terms due to the experiment accuracy.

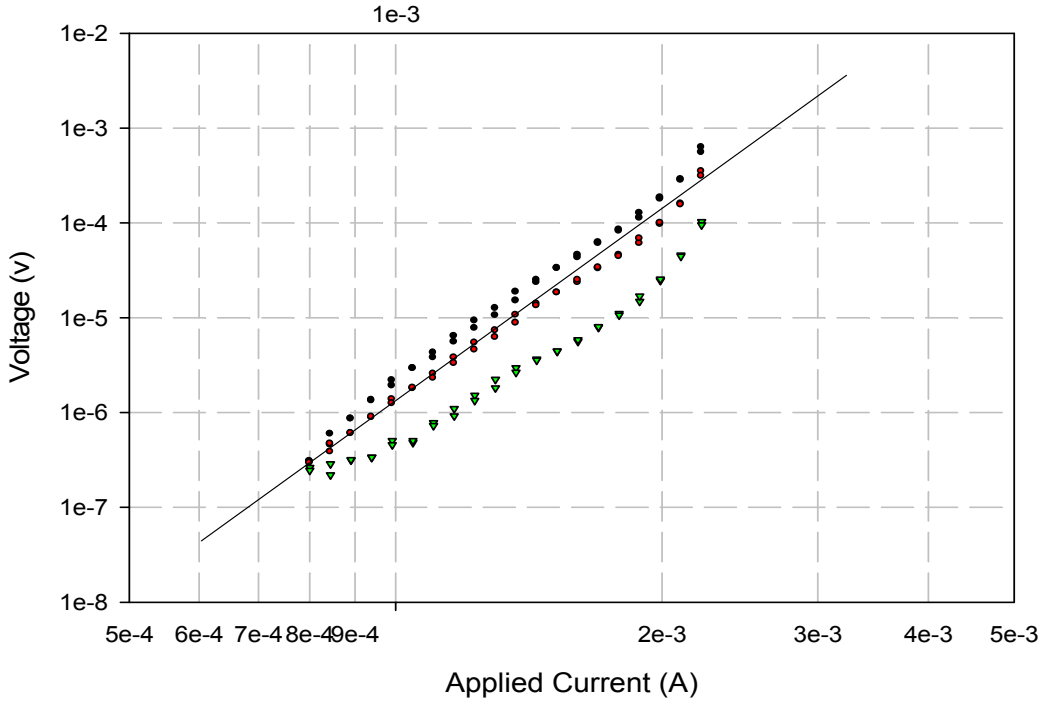

Fig 2.9 I-V characterisc of sample at 3.756K (Sample 4)

Shown in Fig 2.9 is the applied current dependence of the fundamental voltage, the

third harmonic voltage and the fifth harmonic voltage of sample at 3.756K where the power index of current-voltage characteristic is about 7. According to the graph above, the slope of the log-log plot of current-fundamental voltage is close to 7, which is the same as the slope of log-log plot of current-third harmonic voltage and the slope of log-log plot of current-fifth harmonic voltage. The explanation of the experimental result is that the coefficients A, B, C in equation (2.4) are very small, only the fourth term DI^7 plays role at this temperature. According to the trigonometric expanded equation (2.2),

$$\alpha = 7 \qquad V = (\frac{35}{64}\sin(\omega t) - \frac{21}{64}\sin(3\omega t) + \frac{7}{64}\sin(5\omega t) - \frac{1}{64}\sin(7\omega t))I^7$$

there are the fundamental voltage, the third harmonic voltage and the fifth harmonic voltage across the sample, and the power indexes of the log-log plots of current-voltage are seven. The ratio of the fundamental voltage over the third harmonic voltage is supposed to be $35/21 = 1.66$, and the ratio of the fundamental voltage over the fifth

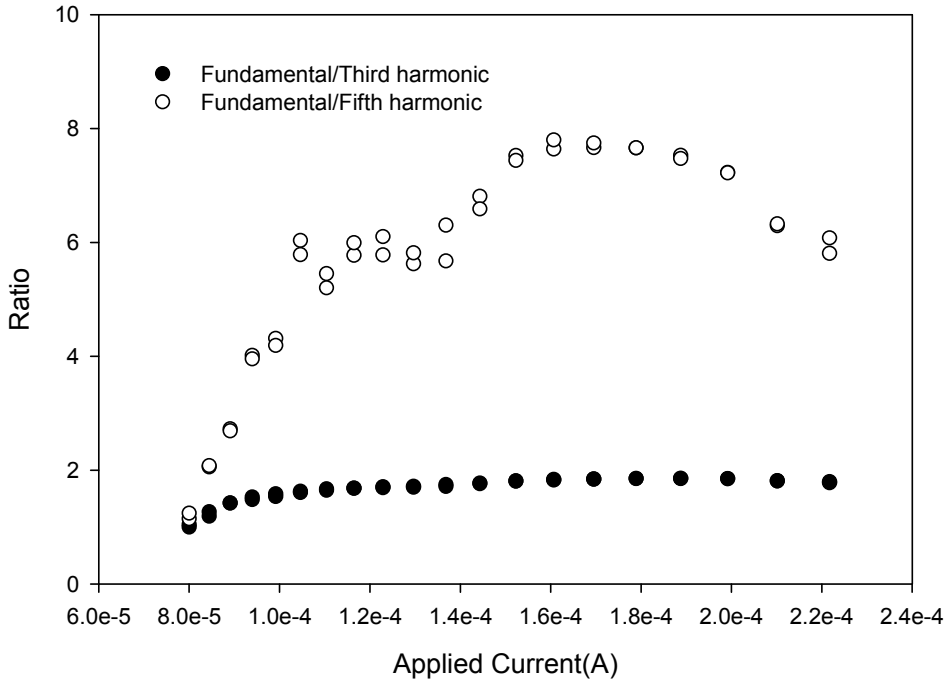

Fig 2.10 The ratio of voltages (Sample 4)

harmonic voltage is supposed to be $35/7 = 5$. Shown in Fig 2.10 are these two ratios of experimental results, which are satisfied with our analysis.

With the increasing temperature, the coefficient of third term in equation (2.4) increases and cannot be neglected any more. Shown in Fig 2.8 where the power index is about 6 gives the similar results to Fig 2.9. But different with the results in Fig 2.9, the term CI^5 in Fig 2.8 is not small any more and plays role with DI^7 together, thus the voltages are the mixture of the trigonometric expansions of CI^5 and DI^7, and all three slopes of current-voltage are the same and about six.

When the temperature reaches 3.765K, the power index is close to 5. At this temperature, the coefficients of the first term and the second term in equation (2.4) is still small, but the coefficient of third term is big enough so that the fourth term can be neglected, i.e., the electrical response in sample at this temperature will be dominated by the vortex pair-pairs in sample.

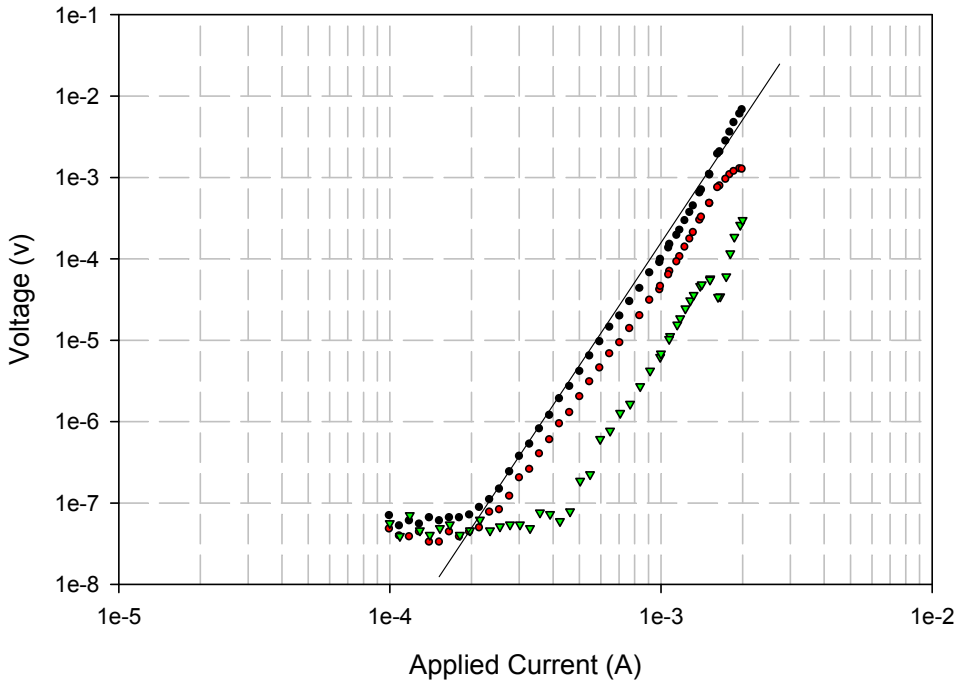

Fig 2.11 I-V characterisc of sample at 3.765K (Sample 4)

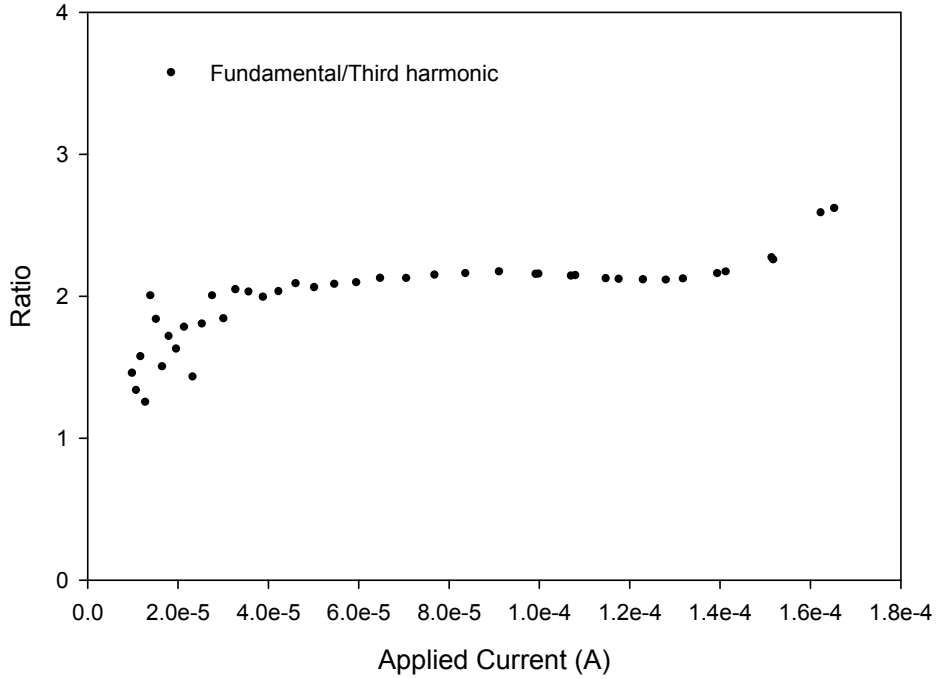

Fig 2.12 The ratio of voltages (Sample 4)

According to the trigonometric expanded equation,

$$\alpha = 5 \qquad V = (\frac{10}{16}\sin(\omega t) - \frac{5}{16}\sin(3\omega t) + \frac{1}{16}\sin(5\omega t))I^5$$

there are the fundamental voltage, the third harmonic voltage and the fifth harmonic voltage across the sample, and the power indexes of current-voltage are same and about five. The experimental results are shown in Fig 2.11 which is satisfied with our analysis. The ratio of the fundamental voltage over the third harmonic voltage is supposed to be $10/5 = 2$. Shown in Fig 2.12 is the ratio of experimental voltages which is satisfied with the result of trigonometric expanded equation above.

At higher temperatures, the second term BI^3 in equation (2.4) increases and becomes comparable with the third term CI^5, which means more and more vortex pairs are separated into the free vortices. According to the trigonometric expanded equation, the fundamental voltage and the third harmonic voltage will be attributed to the second term BI^3 and the third term CI^5 together, thus the slope of log-log plot of

current-fundamental voltage and the slope of log-log plot of current-third harmonic voltage are same and the value is between three and five. But the fifth harmonic voltage only can be attributed to the third term CI^5, so that the slope of log-log plot of current-fifth harmonic voltage is still five which is different with the two others. The experimental results are shown in Fig 2.6 where the power index of current-voltage is four.

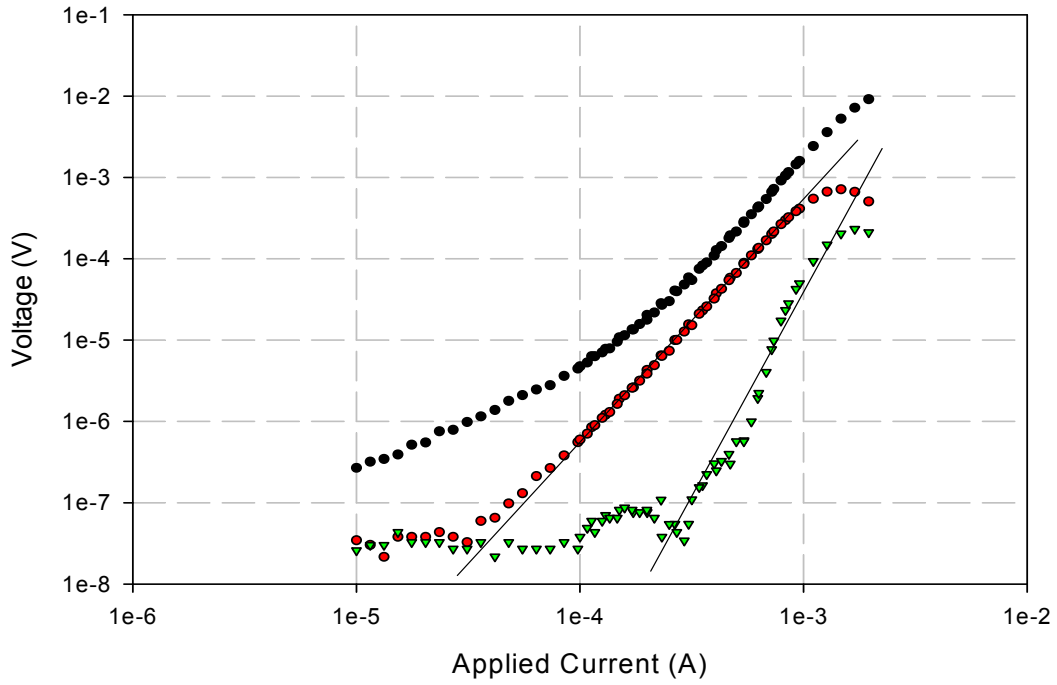

Fig 2.13 I-V characterisc of sample at 3.773K (Sample 4)

The second term BI^3 becomes dominant with further increasing temperature, so the second term will play the main role when the temperature reached 3.773K. At this temperature both the slope of current- fundamental voltage and the slope of current-third harmonic voltage are decided by the second term BI^3 and the values are three, but the slope of current-fifth harmonic voltage are still five. The experimental results shown in Fig 2.13 indicate that second term BI^3 which is attributed to the process of vortex pair separation plays the main role in sample at this temperature. The ratio of the fundamental

voltage over the third harmonic voltage is suppose to be 3 which is satisfied with our experimental results shown in Fig 2.14. The experimental value is a little bigger than 3, which indicates the existence of the first term in equation (2.2). The first term AI is attributed to the motion of free vortices which is produced by the thermal perturbation.

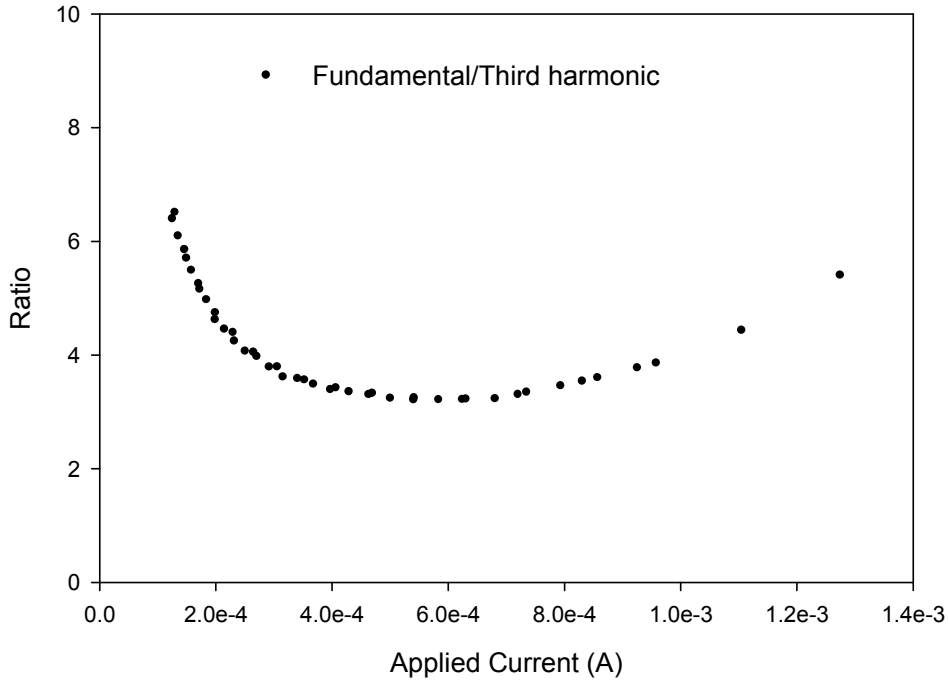

Fig 2.14 The ratio of voltages (Sample 4)

When the temperature continues to increase, the free vortices produced by thermal perturbation will appear in sample. With more and more vortices produced in sample, the first term AI in equation (2.4) will increase and plays an important role in electrical response. This term AI can only contribute to the fundamental voltage. The fundamental voltage will be attributed to the first term AI and the second term BI^3 together, thus the slope of the current-fundamental voltage will be between one and three. The third harmonic voltage is only attributed to the second term BI^3 so the slope of current-third harmonic voltage is still three. The fifth harmonic voltage is smaller compare to the fundamental voltage and the third harmonic voltage, and is only attributed

to the third item CI^5, so the slope of current-fifth harmonic voltage is still five. The experimental results at 3.784K are shown in Fig 2.15.

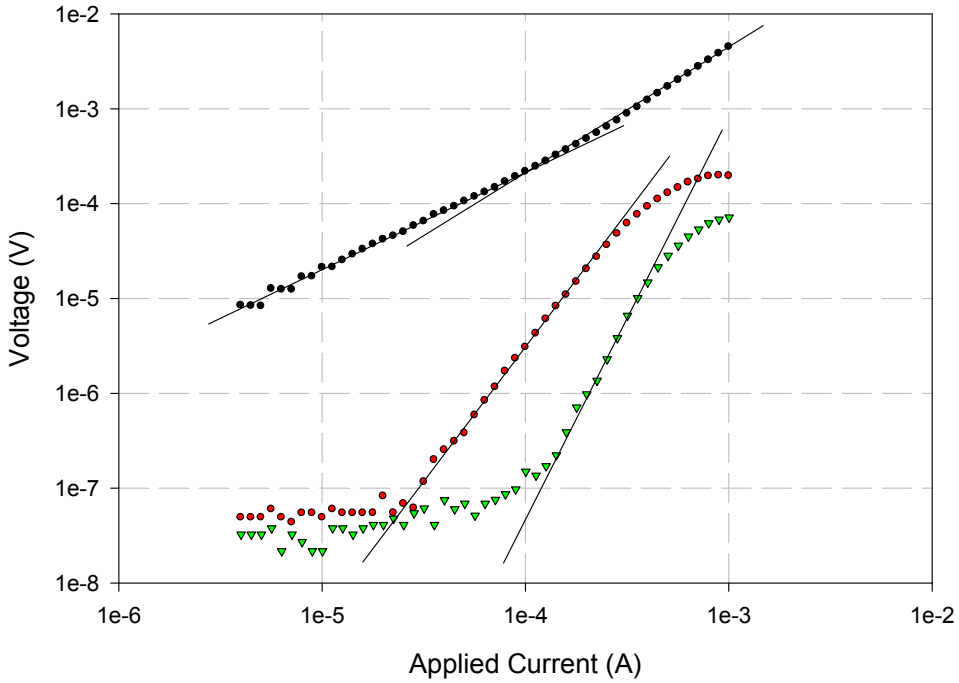

Fig 2.15 I-V characterisc of sample at 3.784K (Sample 4)

2.5 Discussion

According to the analysis in section 2.4, equation (2.4) can describe the vortex motions in superconducting transition in two dimensional samples with the alternating applied current. There are several vortex states in superconducting transition, include the free vortices, vortex pairs, vortex pair-pairs, and the other vortex groups. Typically there are some changes in transition process in two dimensional samples, include the generation and annihilation of free vortices, the separation of vortex pairs and the combination of free vortices, and the generation and the separation of other vortex groups. Shown in Fig 2.16 is the interchange graph of vortex states in the two dimensional

superconducting transition.

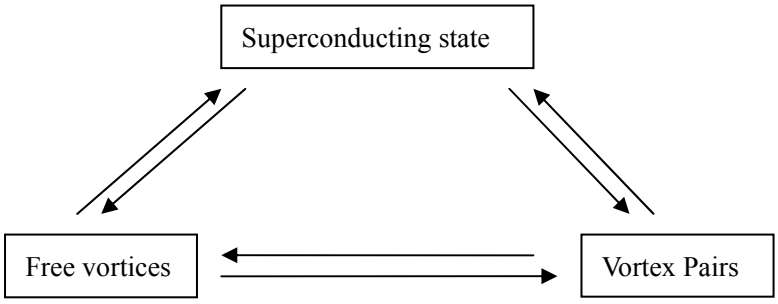

Fig 2.16 The interchange graph of vortex

In equation (2.4), the first term AI is attributed to the motion of free vortices which is generated and annihilated from the superconducting states by the thermal energy or by the applied current. The second item BI^3 is attributed to the process of vortex pair separation which is a reversible process. The third term CI^5 is attributed to the vortex pair-pairs in sample.

During the superconducting transition process, with the increasing temperature, the vortex pair-pairs were produced first and contributed to the term CI^5. Then more and more vortex pairs were produced, and separated into free vortices by the applied current. When the contribution of vortex pair separation process is much more than the contribution of vortex pair-pairs, the third term CI^5 can be neglected and the second term BI^3 will dominate the electrical response of sample. The free vortices will start to be produced by thermal perturbation when the temperature reaches the critical temperature of K-T transition, thus the linear relationship will appear in the current-fundamental voltage characteristics of sample and the slope of log-log plot of current-fundamental voltage at big currents will be less than three. The slope will

decrease with the increasing free vortices in sample until the slope reaches one, where the whole sample turns into the normal state.

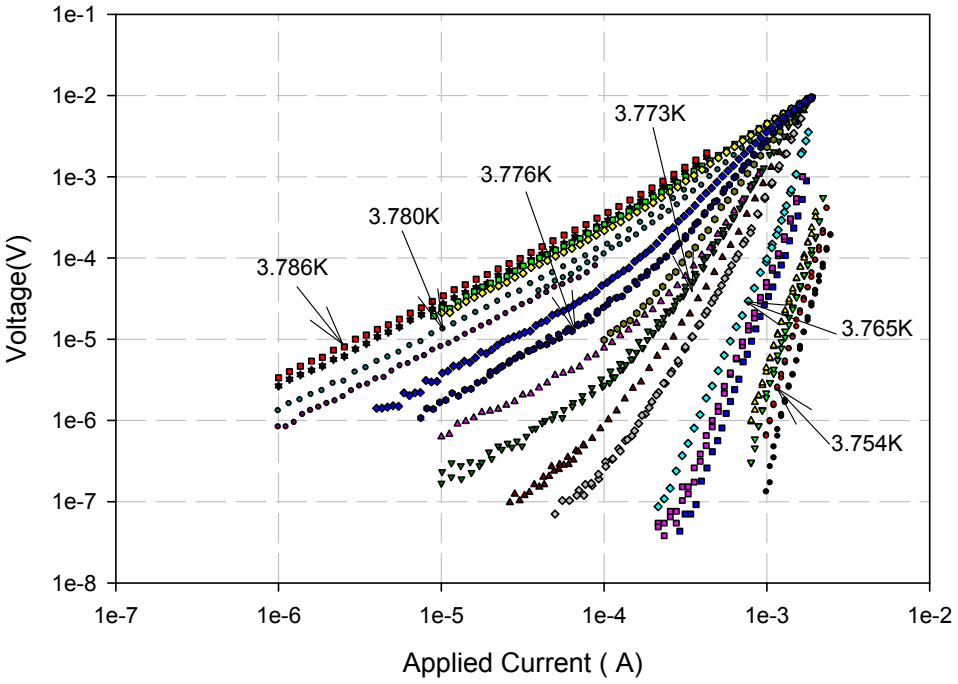

Fig 2.17 The current-fundamental voltage characteristic (Sample 4)

Shown in Fig 2.17 are the current-fundamental voltage characteristics of sample at different temperatures. The graph shows the similar current-voltage characteristics to the graph of direct applied current. At a lower temperature where the resistance is small, $V \propto I^{\alpha}$. At a higher temperature where the resistance is big, $V \propto I$ for small I, and $V \propto I^{\beta}$ for large I. According to equation (2.2) and equation (2.4), the fundamental voltage is given by

$$V = (AI + \frac{3}{4}BI^{3} + \frac{5}{8}CI^{5}) \bullet \sin(\omega t)$$

So in the transition process which is from the superconducting state to the normal state, the fundamental voltage was dominated by the vortex pair-pairs first, then by the separation process of vortex pairs, at last was dominated by the motion of free vortices. The linear relationship of current-voltage for small I at higher temperature was produced

by the first term AI which represents the motion of free vortices. So the current-fundamental voltage characteristic of sample in the alternating applied current can also be used to find out the critical temperature at which the free vortices start to be produced by thermal perturbation, i.e., the critical temperature of K-T transition. However it should be noted that there are other sources that contributed to the linear resistance. One is the existence of earth magnetic field which can generate vortices in sample, thus it is important to shield the earth magnetic field to measure the critical temperature of K-T transition.

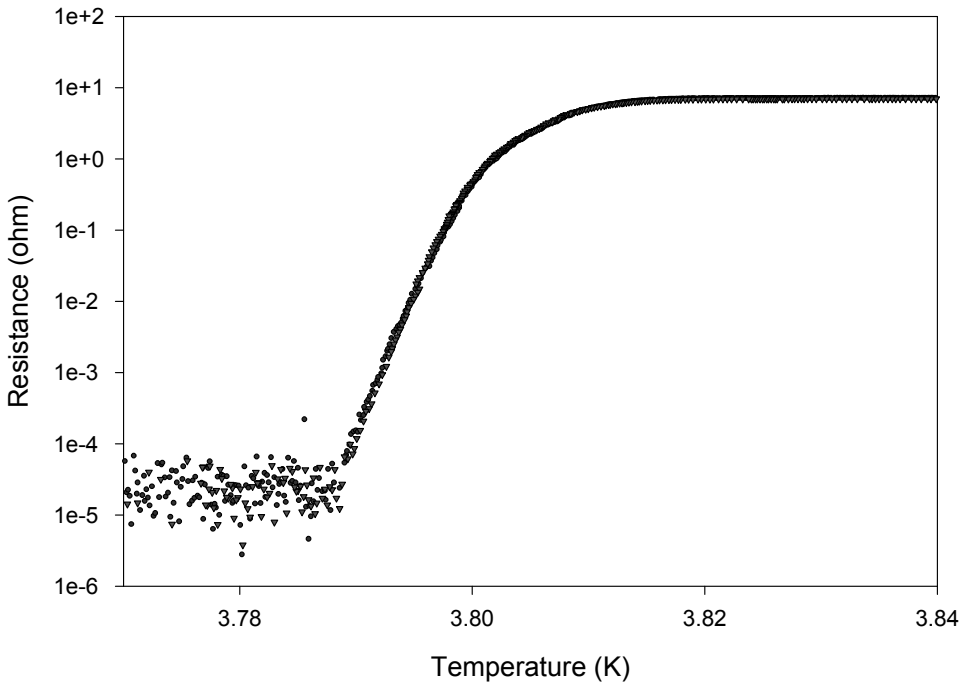

Fig 2.18 Resistive transiton in Log scale R vs T (Sample 4)

If the temperature of sample is higher than the critical temperature of K-T transition, the resistance of sample at small current will be determined by the linear I-V characteristic, which shows the presence of thermally excited free vortices. Theoretical prediction of K-T model gives the dependence near T_c of the form

$$R \propto \exp\{\frac{c}{(T-T_c)^{1/2}}\}$$

Shown in Fig 2.18 is the resistive transition in logarithmical scale resistance as a function of temperature at 50μA. Shown in Fig 2.19 is the logarithm of the resistance as a function of $(T-T_c)^{-1/2}$ where the critical temperature is 3.773K. The plot in Fig 2.19 is fitted well with the theoretical prediction of K-T model.

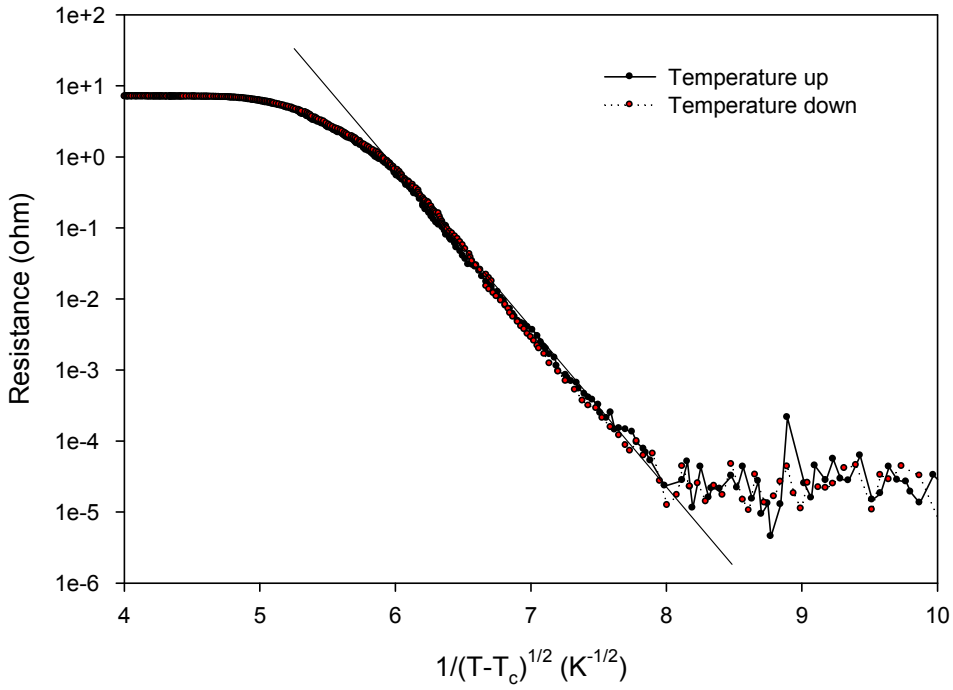

Fig 2.19 Plot for T>T_c of the logarithm of R as a function of $(T-T_C)^{-1/2}$ (Sample 4)

Similar to the discussion above, the critical temperature at which the vortex pairs start to be separated also can be figured out. According to the equation (2.3) and equation (2.4), the third harmonic voltage is given by

$$V = (-\frac{1}{4}BI^3 - \frac{5}{16}CI^5 - \frac{21}{64}DI^7) \bullet \sin(3\omega t)$$

With the increasing temperature, the third harmonic voltage was first dominated by the vortex pair-pairs and other vortex groups, and the slope of log-log plot of current-third harmonic voltage is larger than five. When the vortex pairs start to be separated, the term

BI^3 appears and the slope of current-third harmonic voltage will be less than five. So the temperature at which the slope of current-third harmonic voltage is five is the critical temperature, at which the vortex pairs start to be separated. Above the critical temperature, more and more vortex pairs are produced and separated into the free vortices, the slope of log-log plot of current-third harmonic voltage will decrease with the increasing temperature until it reaches three. Shown in Fig 2.20 are the current-third harmonic voltage characteristics of sample at different temperatures. The line in the graph where the slope is five indicates the critical temperature is 3.763K.

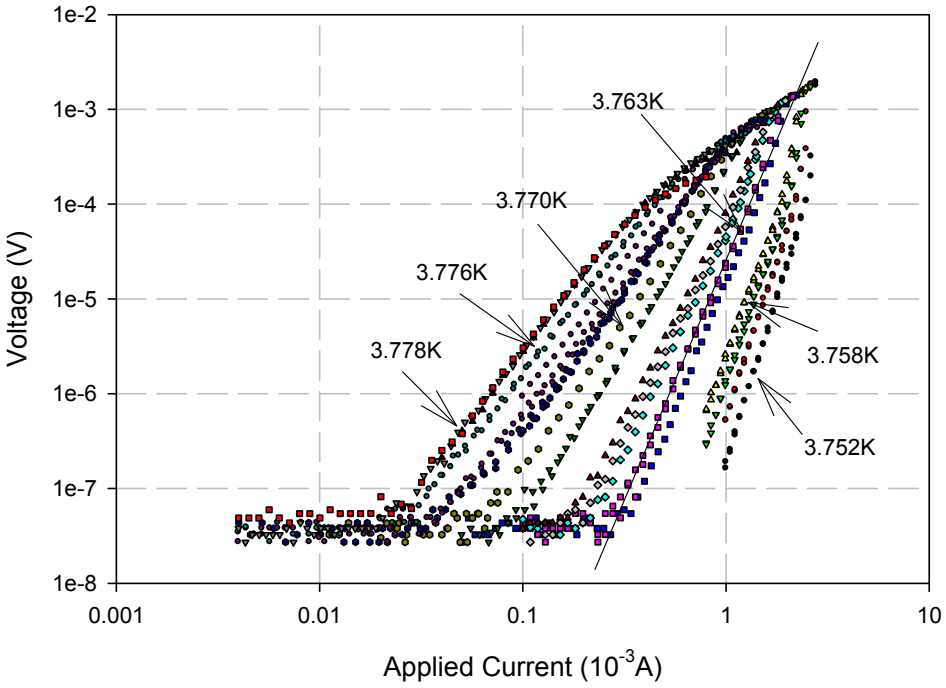

Fig 3.20 The current-third harmonic voltage characteristic (Sample 4)

Chapter 3 Excess Noise in Tin Film

3.1 Measurement Accuracy

In our noise measurement, the noise signals were first fed into SR554 low noise transformer preamplifier and followed by two stages of SR560 low noise preamplifiers. The noises were measured typically at 1 KHz and the total amplification is 10^5. All of the measurement instruments were set in a faraday shield to minimize external electrical fields. But there was still background noise recorded in the SR760 spectrum analyzer, so it is necessary to discriminate the noise signals from the background noise. The measurement accuracy of noise signals not only depends on the sensitivity of instruments, but also depends on the level of the background noise.

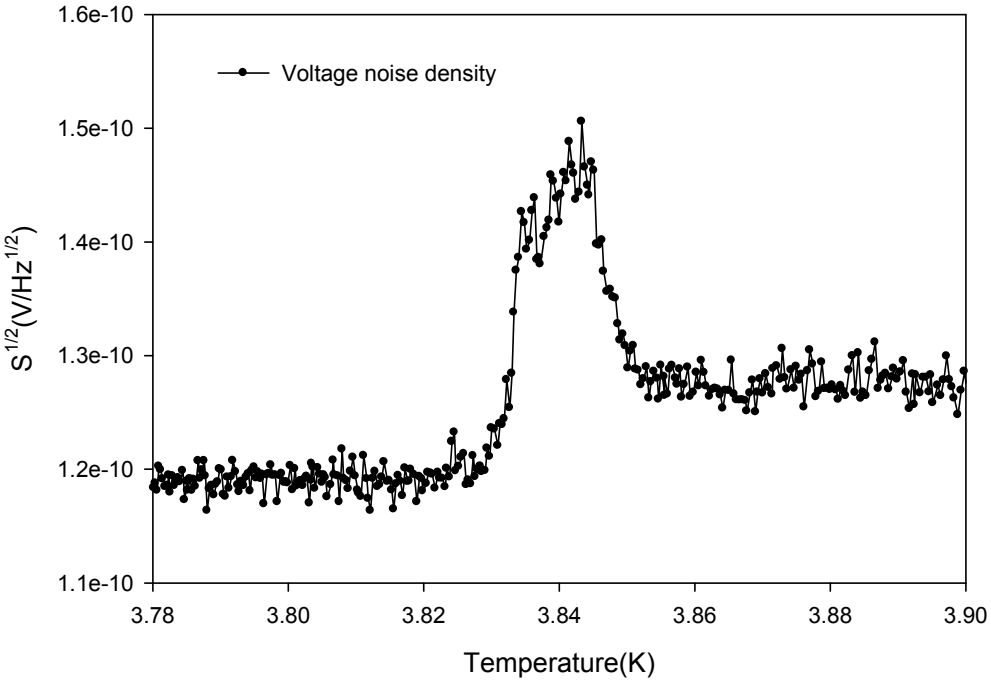

Fig 3.1 The temperature dependence of voltage noise density (Sample 17)

Shown in Fig 3.1 is the temperature dependence of the voltage noise density $S^{1/2}$. The voltage noise density below the superconducting transition is the background noise,

and the voltage noise density above the superconducting transition is the mixture of the background noise and the Johnson noise which is produced by the thermal fluctuation of the resistance of sample. The voltage noise density in the superconducting state in Fig 3.1 is about $1.19\times10^{-10}V/Hz^{1/2}$

The noise power of sample can be estimated by subtracting the background noise,

$$S' = S - S_{background}$$

Shown in Fig 3.2 is the temperature dependence of the voltage noise density $S^{1/2}$ without the background noise. The voltage noise density above the superconducting transition process is $4.6\times10^{-11}V/\sqrt{Hz}$ which is close to the Johnson noise $\sqrt{4K_BTR} = 2.7\times10^{-11}V/\sqrt{Hz}$

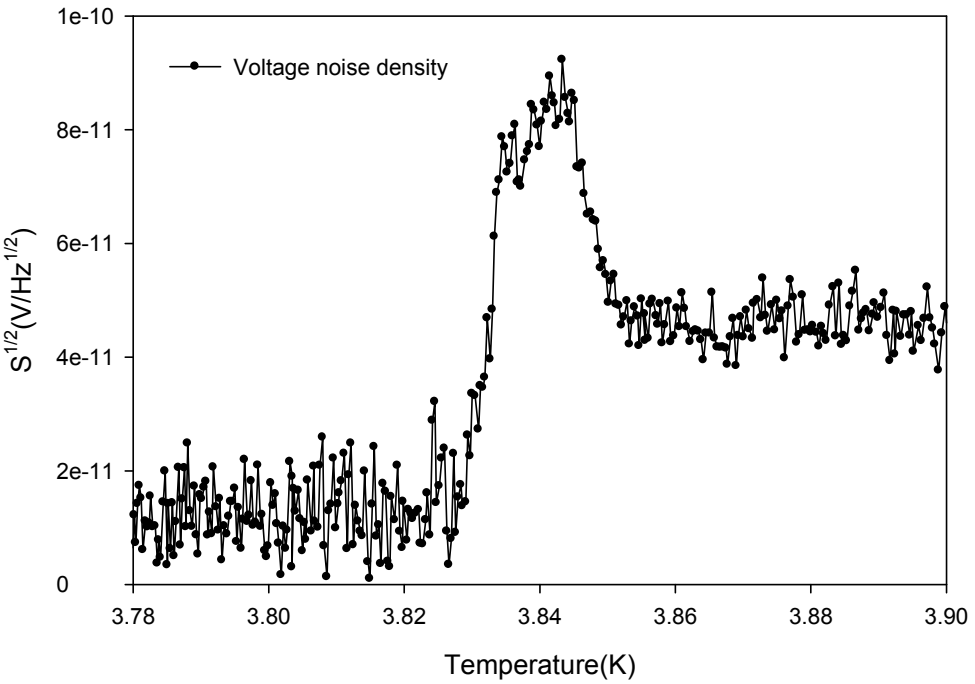

Fig 3.2 The voltage noise density without the background noise (Sample 17)

According to the discussion above, the measurement accuracy of our experiment is good enough to measure the noise signals in our experiment which varies from $0.1-10nV/\sqrt{Hz}$.

3.2 Excess Noise with AC

Shown in Fig 3.3 is the temperature dependence of the resistance of Tin film in superconducting transition. The critical temperature of superconducting transition is about 3.81K and the transition width is about 25mK. The data shown here are taken when both the temperature is slowly pumping down and slowly drifting up. The resistance of this Tin film in normal state at 4K is about 7ohm.

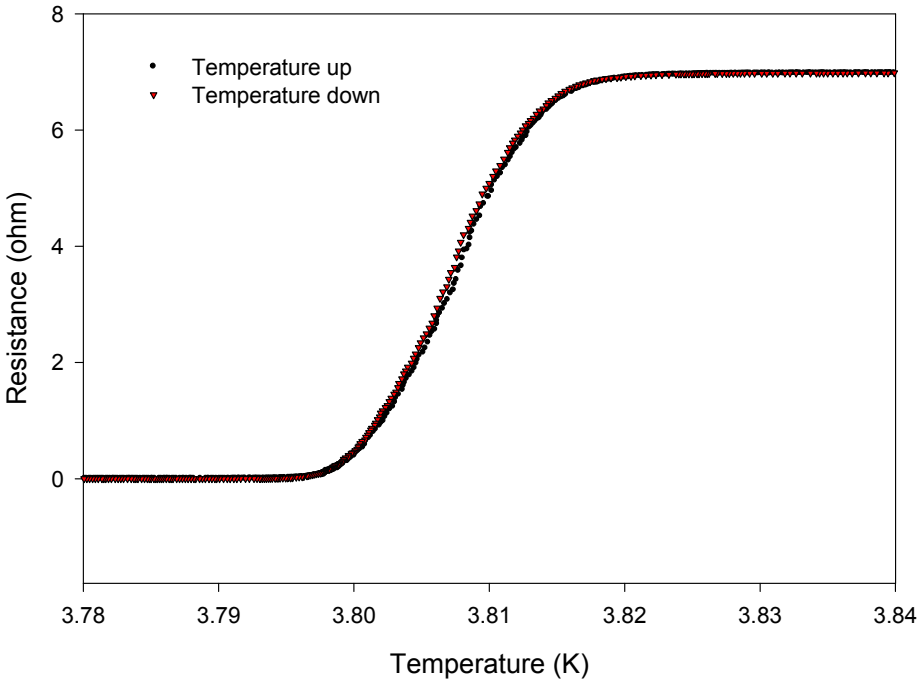

Fig 3.3 The temperature dependence of Resistance (Sample 4)

Shown in Fig 3.4 is the temperature dependence of the voltage noise density with a $50\mu A$ alternating current. The applied current is at 16Hz and the noise is measured at 1 KHz. The noise was measured when both the temperature is slowly pumping down and slowly warming up. The temperature decreasing rate is higher than the increasing rate, but the two curves in Fig 3.4 are almost coincided so that the amplitude of noise is independent on the temperature drifting rate. Fig 3.4 shows that the voltage noise density $S^{1/2}$ is strongly peaked in the superconducting transition.

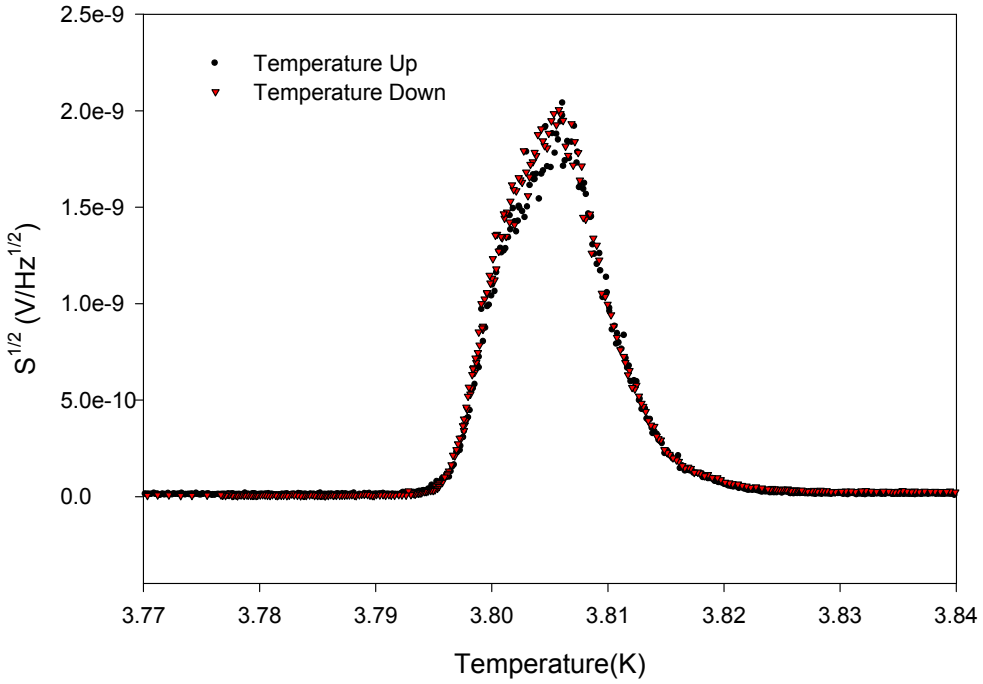

Fig 3.4 The temperature dependence of voltage noise density (Sample 4)

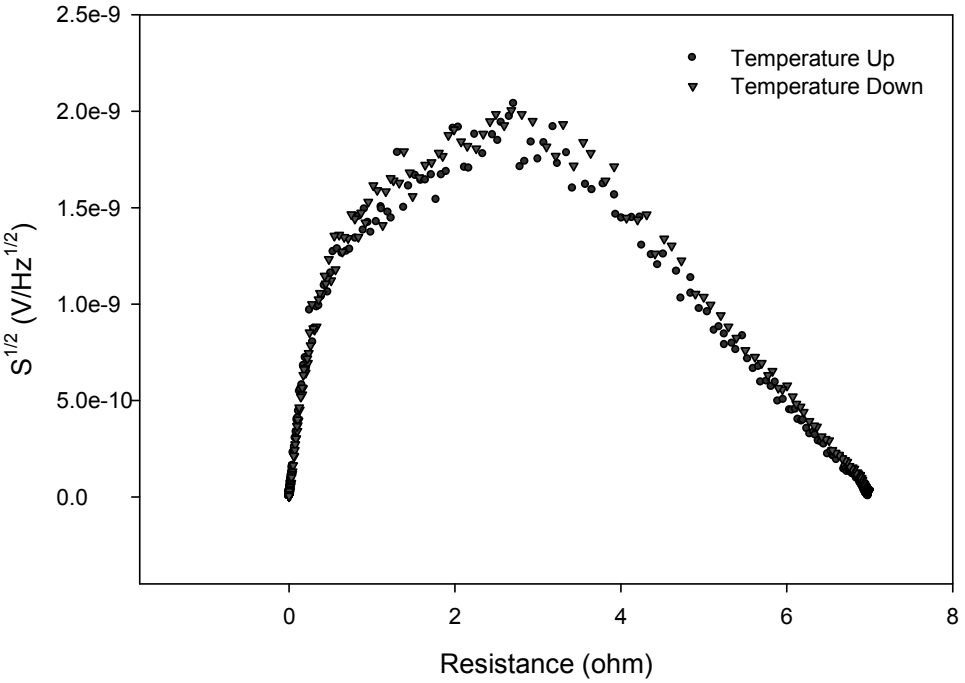

Fig 3.5 Noise versus Resistance (Sample 4)

One of the sources of excess noise is the flux noise which is related with the number of free vortices in samples, i.e., the excess noise is strongly related with the resistance of sample. Shown in Fig 3.5 is the plot of voltage noise density as a function of

resistance for the entire transition. It is clear from the graph that the voltage noise density increases with the increasing resistance initially, i.e., the voltage noise density increases with the increasing number of free vortices. The noise voltage density reaches a peak and decreases with the increasing resistance after the peak. The decreasing of noise is due to the increasing interaction of vortices at high vortex density in sample, which depresses the vortex fluctuation and decreases the flux noise.

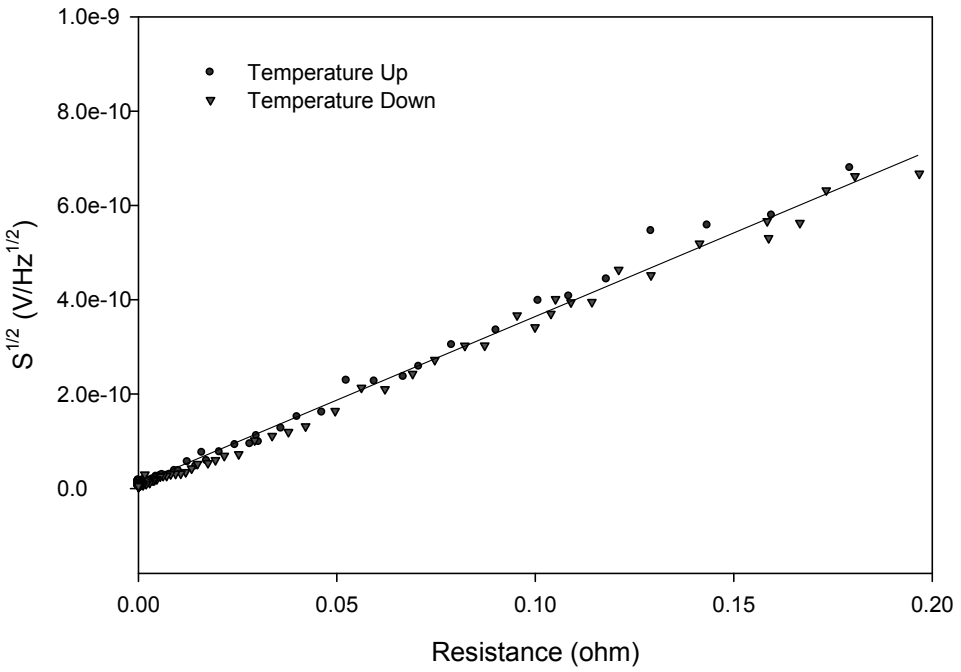

Fig 3.6 The linear relationship between noise and resistance for samll R (Sample 4)

The excess noises depend strongly on the resistance and the excitation current. For a small resistance R<0.2ohm, Fig 3.6 shows the voltage noise density $S^{1/2}$ is clearly linear with R, which means the voltage noise density is linear with the number of free vortices at the lower temperature in the superconducting transition, i.e.,

$$S^{1/2} = AR \qquad (R < 0.2\Omega)$$

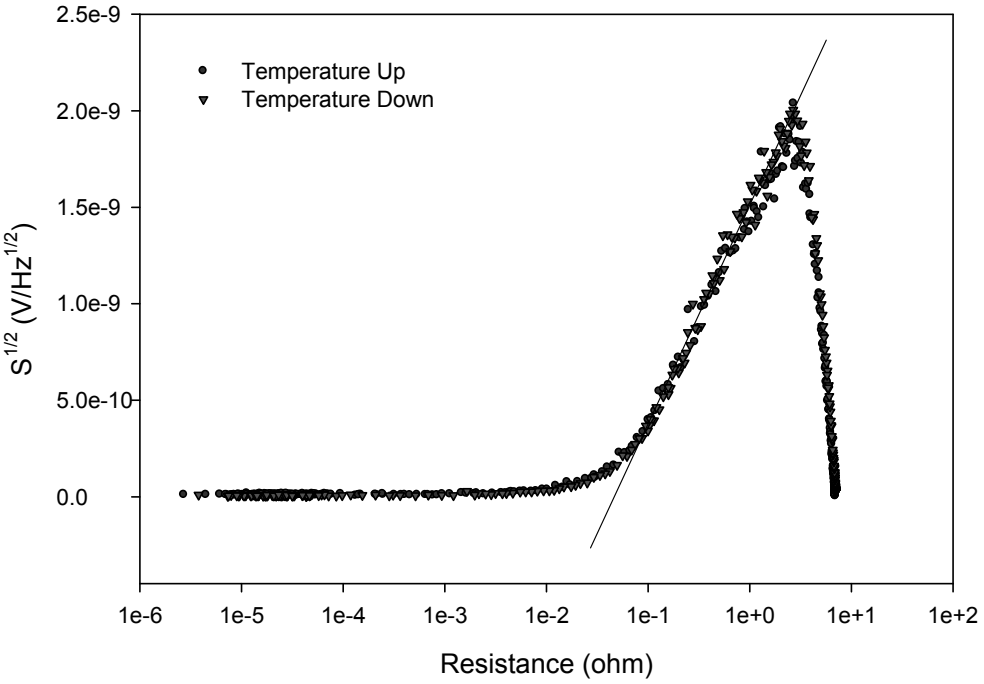

Fig 3.7 Noise vs Log Resistance (Sample 4)

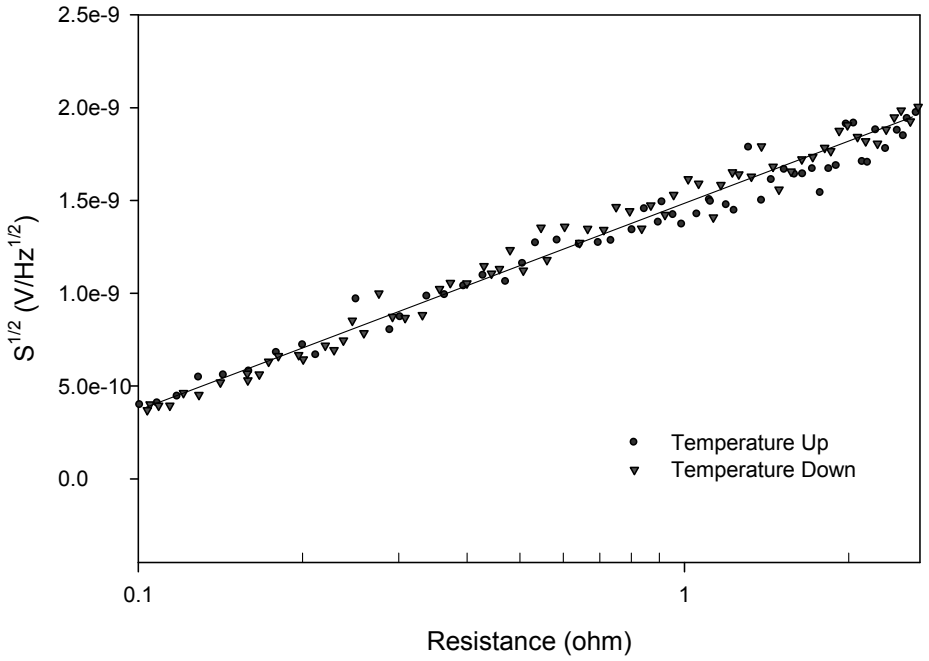

Fig 3.8 The linear relationship between noise and logarithmical resistance (Sample 4)

For a big resistance R>0.2ohm, if the log scale is used to plot the resistance, the voltage noise density $S^{1/2}$ will be linear with the logarithmical resistance for the intermediate resistance which is between 0.2ohm and 3.0ohm. Shown in Fig 3.7 is the plot of voltage noise density as a function of logarithmical resistance for the entire

transition. Shown in Fig 3.8 is the expanded view of the linear relationship between the voltage noise density and the logarithmical resistance for the intermediate resistance. So the empirical equation for the intermediate resistance will be given by,

$$S^{1/2} = B\log(R) \qquad (0.2\Omega < R < 3\Omega)$$

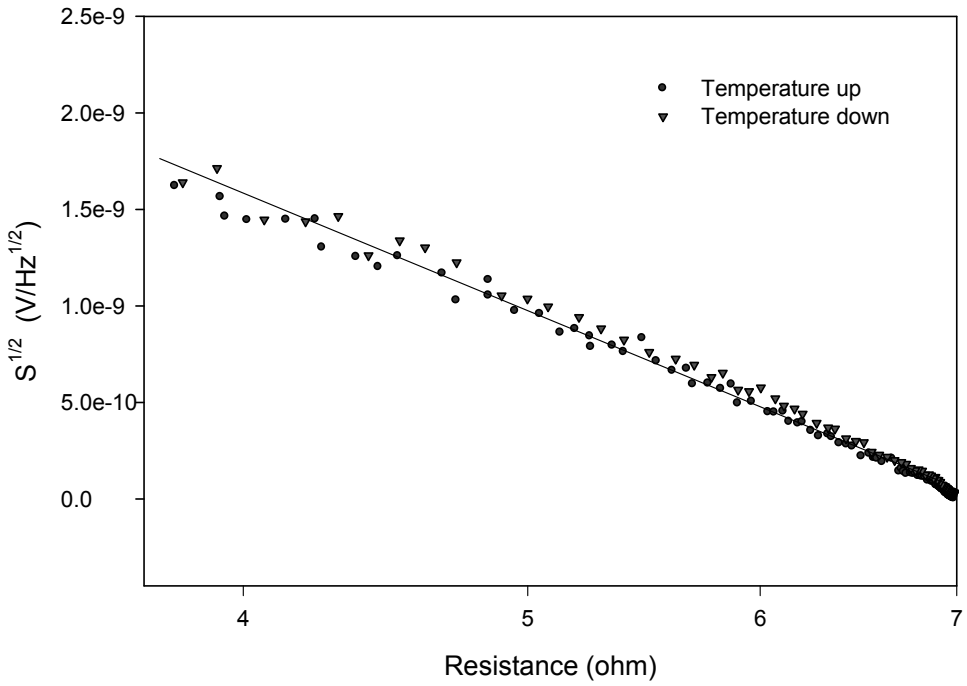

Fig 3.9 Noise vs Resistance after the peak (Sample 4)

After the peak when the sample is close to the normal state, the excess noise decreases rapidly with the increasing resistance. The data can be fitted to either linear or logarithmic resistance dependence. Shown in Fig 3.9 is the linear relationship between the noise and the resistance after the noise peak, that is,

$$S^{1/2} = CR \qquad (R > 3\Omega)$$

According to the discussion above, the empirical results of voltage noise density with ac current in superconducting transition in term of resistance for the entire transition will be given by,

$$S^{1/2} = \begin{cases} AR & R < 0.2\Omega \\ B\log(R) & 0.2\Omega < R < 3\Omega, \ \textit{before the peak} \\ CR & R > 3\Omega, \ \textit{after the peak} \end{cases} \qquad (3.1)$$

where the resistance values which give the intervals of function (3.1) depend on the resistance of sample in normal state. This function is just an empirical function which is suitable with the different alternating applied currents. Shown in Fig 3.10 is an overlay of the plots of voltage noise density versus logarithmical resistance for different applied alternating currents. The plots in Fig 3.10 show that equation (3.1) is satisfied with the different applied alternating currents.

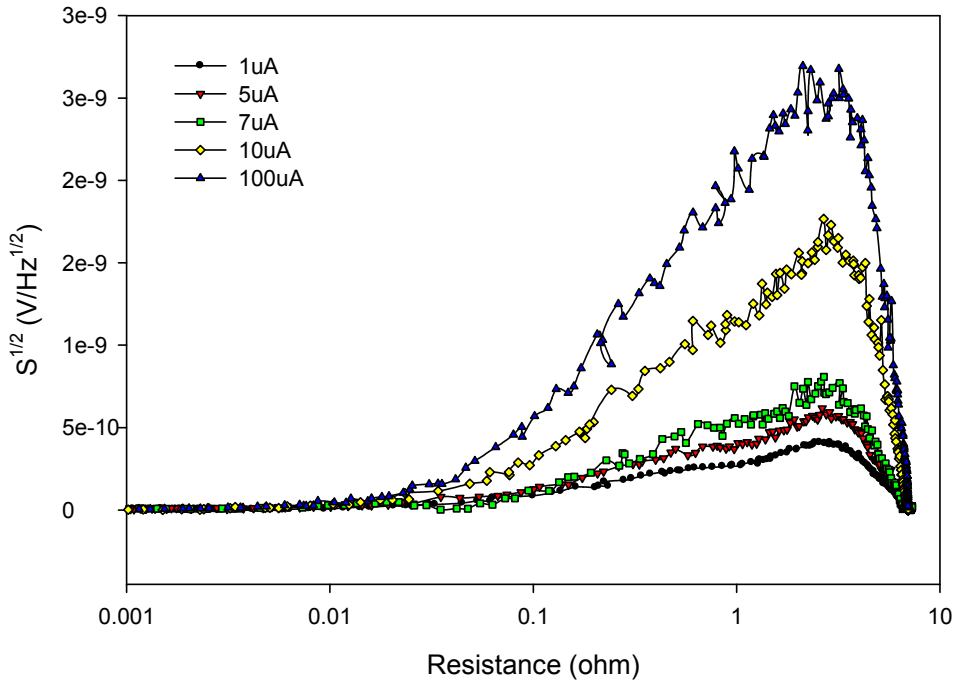

Fig 3.10 Noise vs Logarithmical Resistance for different currents (Sample 4)

Since the voltage noise is supposed to be linear with the fluctuation of the resistance of sample, the voltage noise should be related with the change rate of resistance. The resistance of sample depends on the temperature in the transition process and the sensitivity can be characterized by dR/dT. If dR/dT is big which means the resistance of sample is easy to change with the temperature, the fluctuation of resistance at this

temperature should be big, and the voltage noise of sample at this temperature is big too. Shown in Fig 3.3 is the temperature dependence of the resistance which can be fitted by the equation,

$$R = R_0 + \frac{a}{(1+e^{-\frac{T-T_0}{b}})^c}$$

Then the derivative of resistance dR/dT will be given by,

$$\frac{dR}{dT} = \frac{ac}{b}(1+e^{-\frac{T-T_0}{b}})^{-c-1} e^{-\frac{T-T_0}{b}}$$

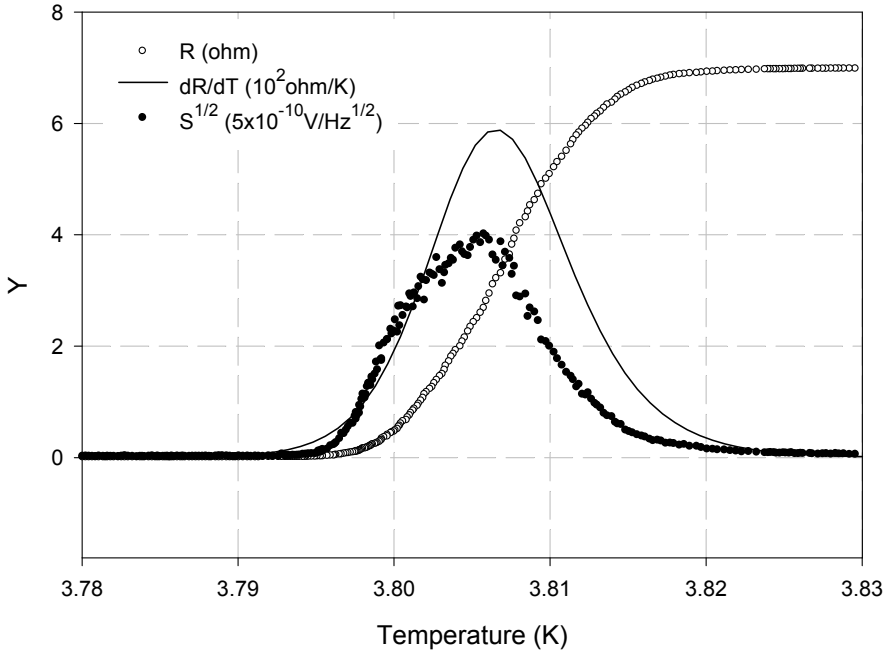

Fig 3.11 The temperature dependece of the $S^{1/2}$ and dR/dT and R at 50uA (Sample 4)

Shown in Fig 3.11 is an overlay of the temperature dependence of the voltage noise density $S^{1/2}$, the resistance R and the derivative of resistance dR/dT during the transition at $50\mu A$. The dR/dT is multiplied by 10^{-2}, and the voltage noise density is multiplied by $2x10^9$ to be displayed on the same scale as resistance. Both the voltage noise density and the derivative of resistance are strongly peaked during the transition. The peak of the voltage noise density is a slightly shifted toward lower temperature from the peak of the

derivative of resistance. The reason of this shift is that the noise is not only attributed to the fluctuation of the number of free vortices which is produce by thermal perturbation, but also to the fluctuation of the separation process of vortex pairs and affected by the interaction of vortices. This shift is also observed in the earlier work in Tin films with direct applied currents by Konedler et al in 1983 [40].

3.3 Excess Noise Comparison between AC and DC

The excess noises in superconducting transition in two dimensional Tin films with alternating currents are discussed in last section. An interesting topic is to compare the excess noises between with the alternating current and with the direct current, which will help us to understand the excess noises better. Shown in Fig 3.12 is an overlay of the temperature dependence of the voltage noise density with alternating current and with direct current at 100μA. Both of them are strongly peaked during the transition, but the peak of the voltage noise density in alternating applied current is much bigger than the peak in direct applied current.

The reason of such big difference is possibly attributed to the separation process of vortex pairs in the transition. When a direct current is applied, the excess noise is produced by the fluctuation of the number of free vortices, which is produced by the thermal perturbation or the fluctuation of the vortex pair separation process. Since the depairing process and pairing process exist in the sample at the same time, the vortex pair separation process in transition is a reversible dynamic process while it is quasi-static for

a constant direct excitation current. The fluctuation of the vortex pair separation process is small in the case of direct applied current. When an alternating current is applied, some vortex pairs are separated by the current when the current is increased, and paired again when the current is reduced. The reversible process is not balanced any more. The number of vortex pairs and the number of free vortices fluctuate with the applied current. The fluctuation of vortex pair separation process with ac currents will be big and the voltage noise density will be big too. The experimental results shown in Fig 3.12 suggest that the vortex pair separation process is very important to understand the source of excess noise.

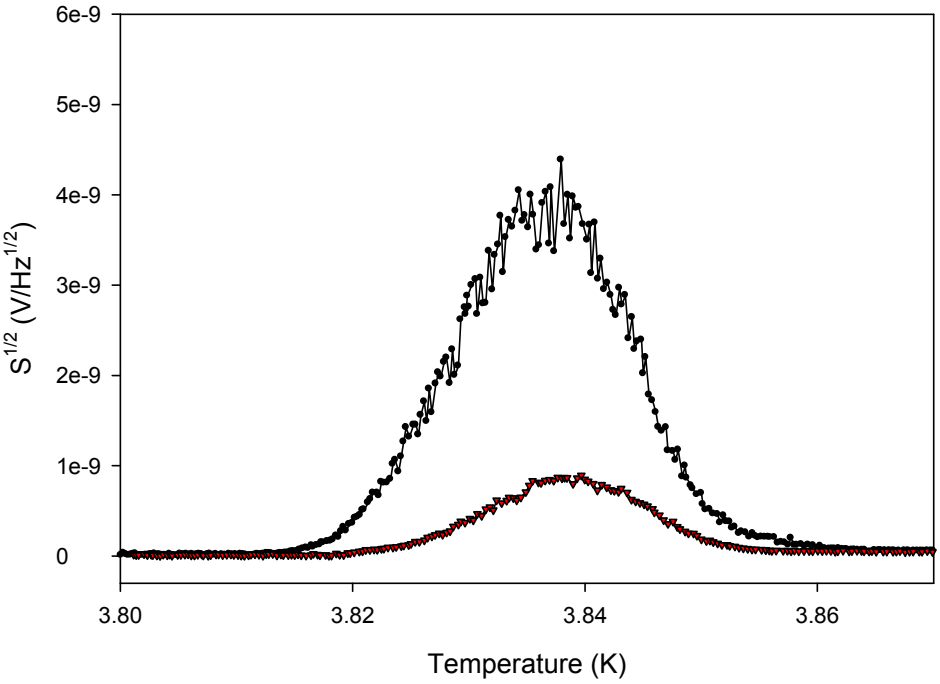

Fig 3.12 The temperature dependence of $S^{1/2}$ at 100uA (Sample 17)

To compare the two curves in Fig 3.12, the voltage noise density with dc is multiplied by 4.5 to be comparable with the voltage noise density with ac. Shown in Fig 3.13 is the comparison of these two curves. The temperature dependences of voltage noise density at 10uA are also compared between ac and dc. Shown in Fig 3.14 is the

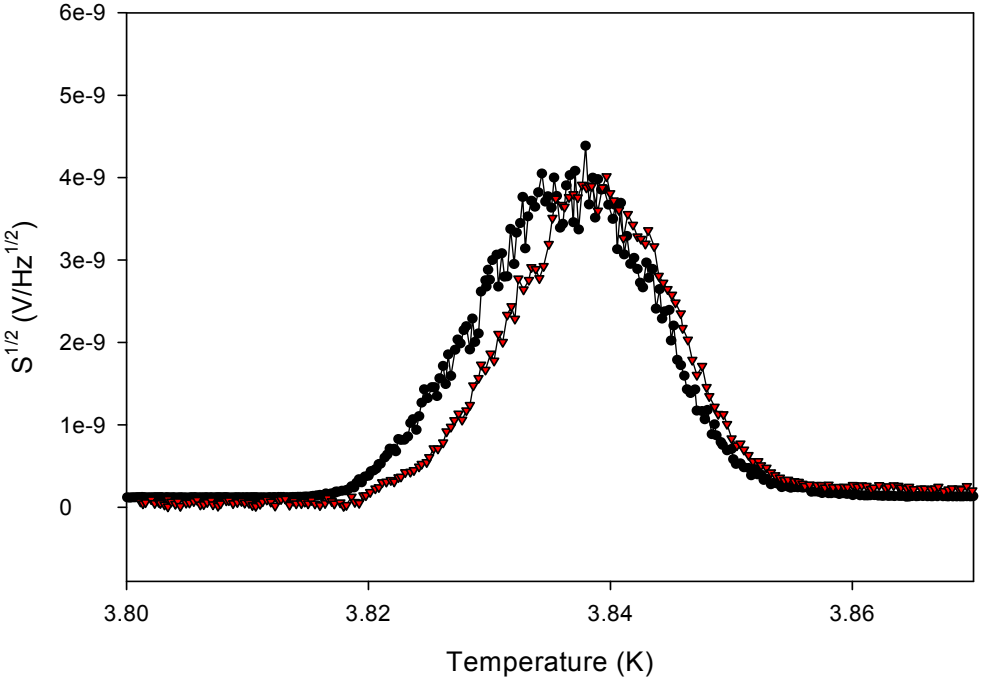

Fig 3.14 The temperature dependence of $S^{1/2}$ at 100uA (Sample 17)

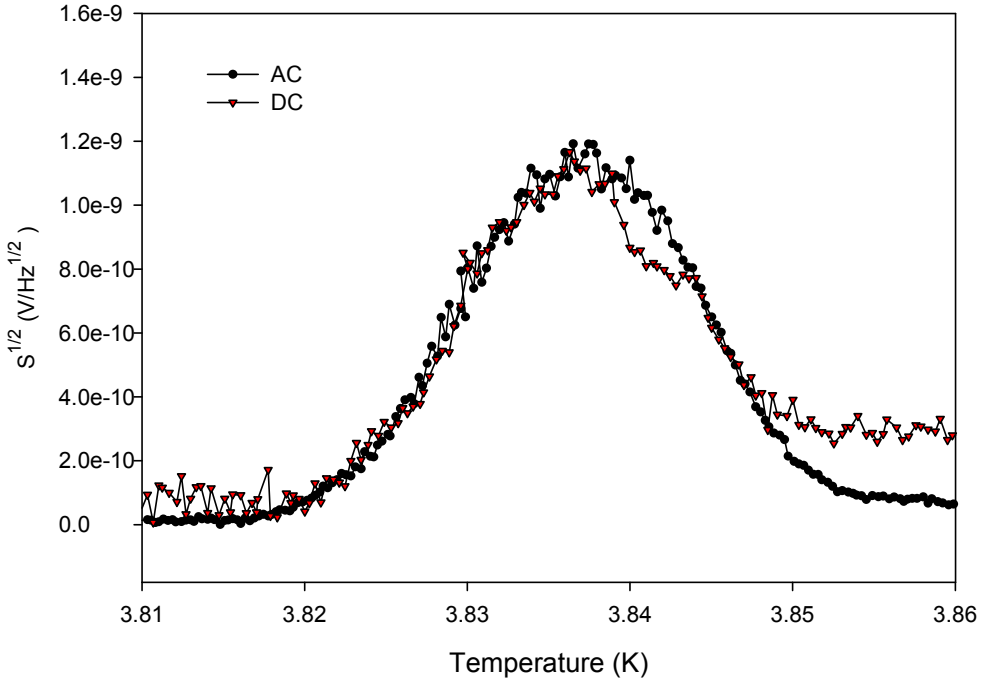

Fig 3.15 The temperature dependence of the $S^{1/2}$ at 10uA (Sample 17)

comparison of the voltage noise densities between ac current and dc current at 10μA. The match between the two data sets in Fig 3.14 are better than the curves in Fig 3.13 because at small current, the noise produced by the thermal perturbation is comparable with the

noise produced by the fluctuation of the vortex pair separation process, both of these fluctuations exist in sample. At big current, the noise associated with ac current is dominated by the fluctuation of the vortex pair separation process, thus resulting in a shift in its temperature dependence from that of dc.

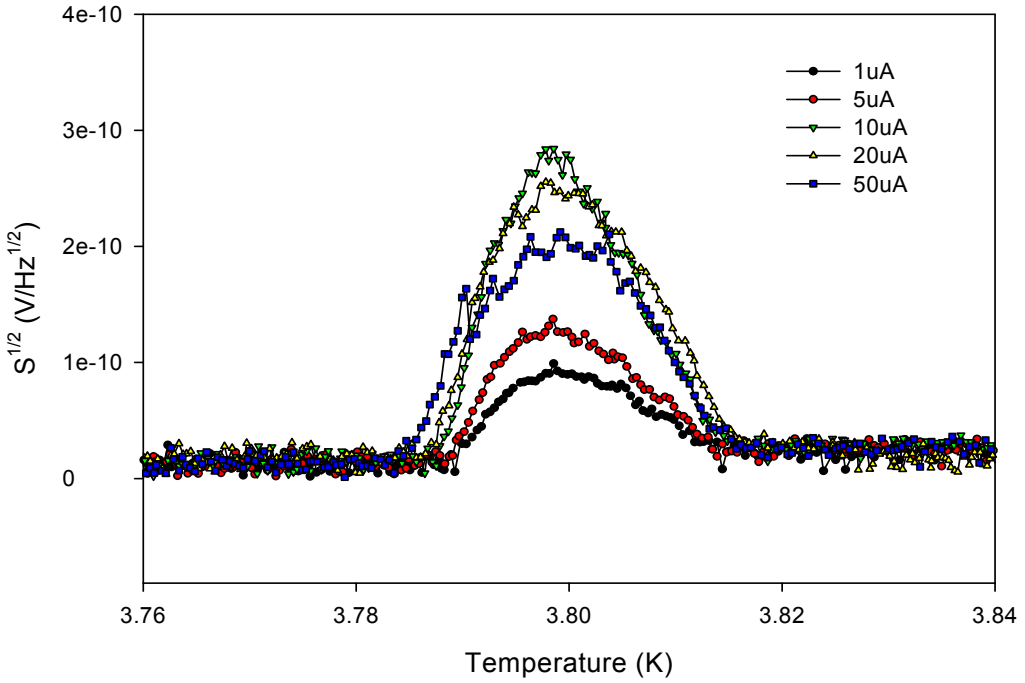

Fig 3.15 The temperature dependence of the $S^{1/2}$ in DC (Sample 14)

According to the discussion above, the excess noises with direct currents are mainly produced by the thermal perturbation and the small fluctuation of the vortex pair separation process. However for alternating excitation currents, only when the current is very small, the noise generation is similar as the case of dc. When the current is big, the noise is mainly produced by the fluctuation of the vortex pair separation process which is perturbed by the applied current. For most range of current, the voltage noise density should be strongly related with the amplitude of excitation current, i.e., the voltage noise density with ac is more sensitive to the current variations than the voltage noise density with dc at big currents. Shown in Fig 3.15 is the temperature dependence of the voltage

noise density with dc at different currents. Shown in Fig 3.16 is the temperature dependence of the voltage noise density with ac at different currents.

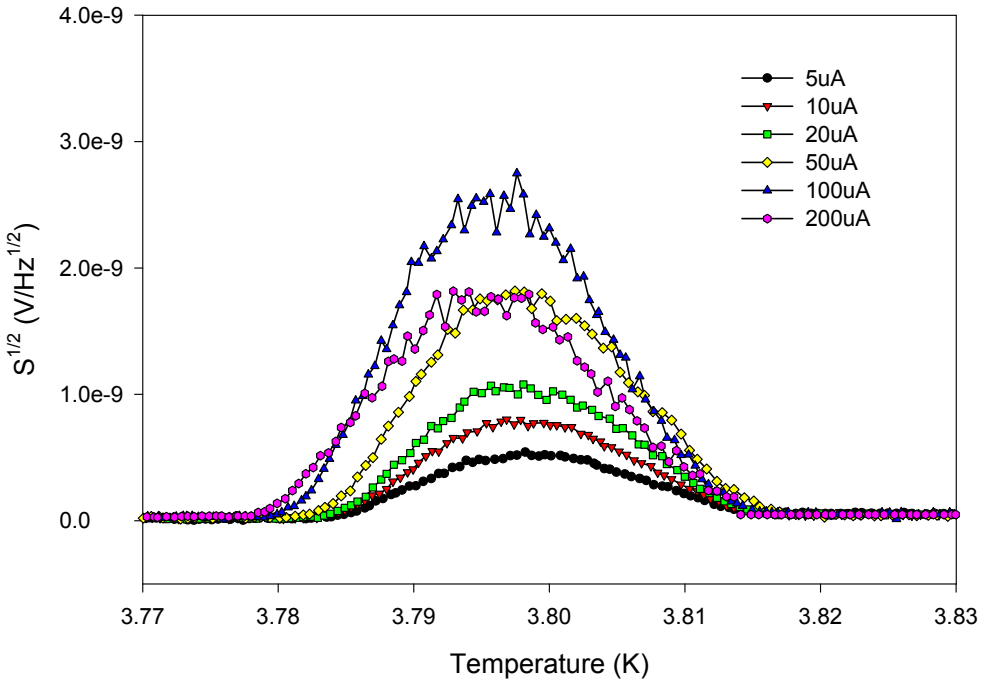

Fig 3.16 The temperature dependence of the $S^{1/2}$ in AC (Sample 14)

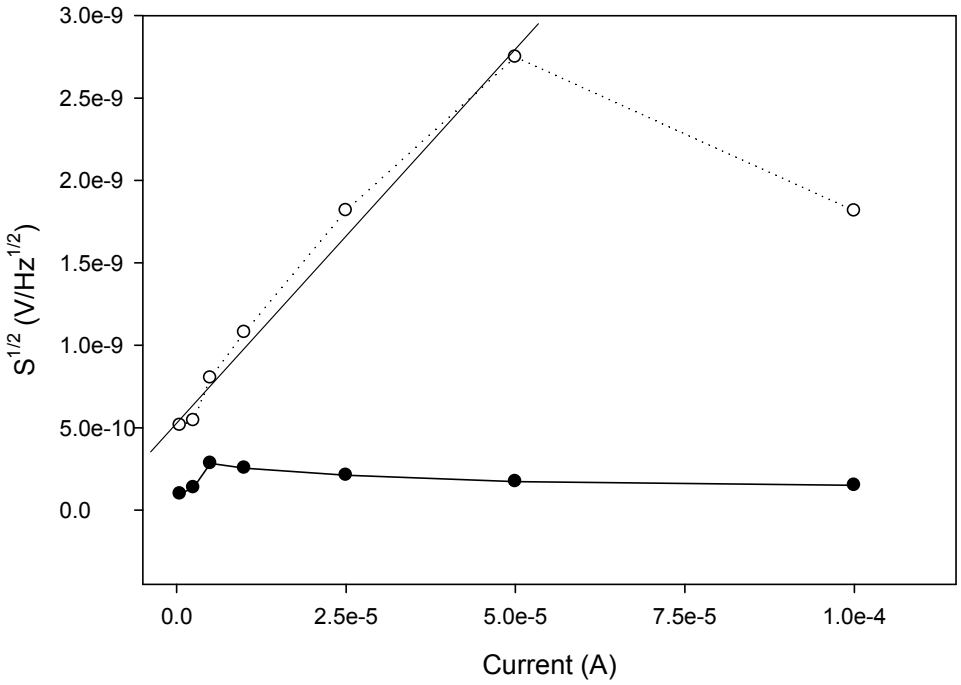

Fig 3.17 The current dependence of the peak of $S^{1/2}$ (Sample 14)

Shown in Fig 3.17 is the current dependence of the peak of voltage noise density.

The plots show that the peak of voltage noise density with ac is more sensitive to the current variations than the peak of voltage noise density with dc for most range of current. The peak of voltage noise density with ac is linear with the excitation current, which indicates that the alternating applied currents dominate the noise production for the intermediate current. The reason of the voltage noise density peak decreasing with the increasing current at very big excitation currents is that the increasing interaction of vortices will depress the fluctuation of vortex pair separation process and decrease the voltage noise density. Similarly, Fig 3.17 suggests that the fluctuation of vortex pair separation process is an important source of the excess noises in two dimensional samples.

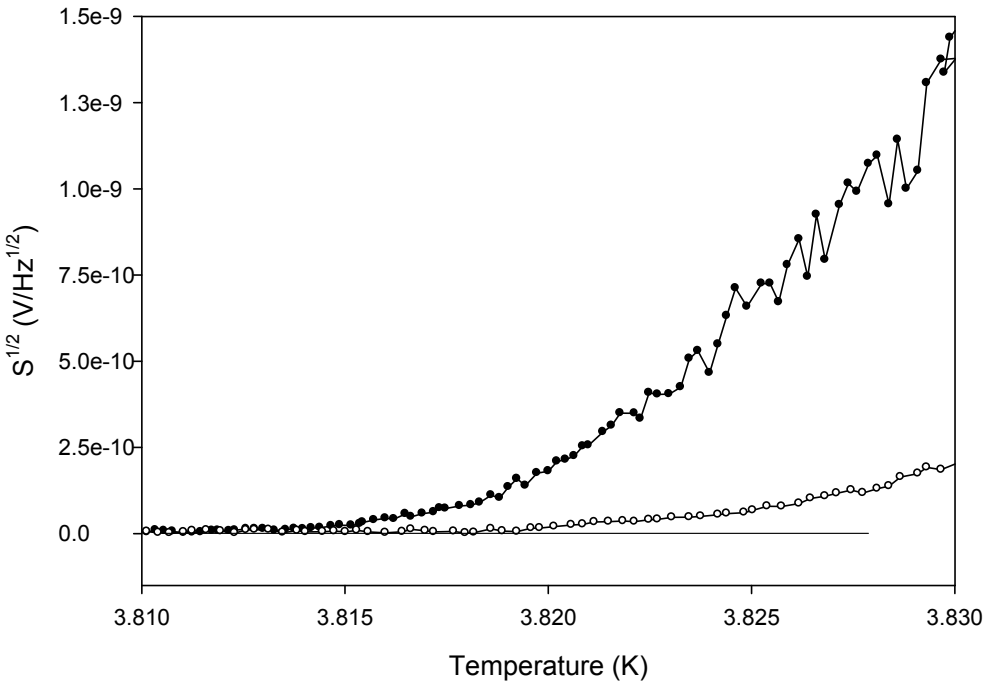

Fig 3.18 The temperature dependence of $S^{1/2}$ at lower T (Sample 17)

At the low temperature side of superconducting transition, the number of free vortices produced by thermal perturbation is small so that the fluctuation of the number of free vortices can be neglected. There is no excess noise with direct applied currents in

sample at this temperature. However, appreciable vortex noise due to the fluctuation of the vortex pair separation process can be measured at this temperature when an alternating current is applied. Shown in Fig 3.18 is the temperature dependence of the voltage noise density at lower temperature at 100μA. The plots show that with the increasing temperature, the excess noise appears first in the alternating current, which is produced by the fluctuation of the vortex pair separation process. The excess noise with the direct current appears at a higher temperature than that of ac in support of our analysis above.

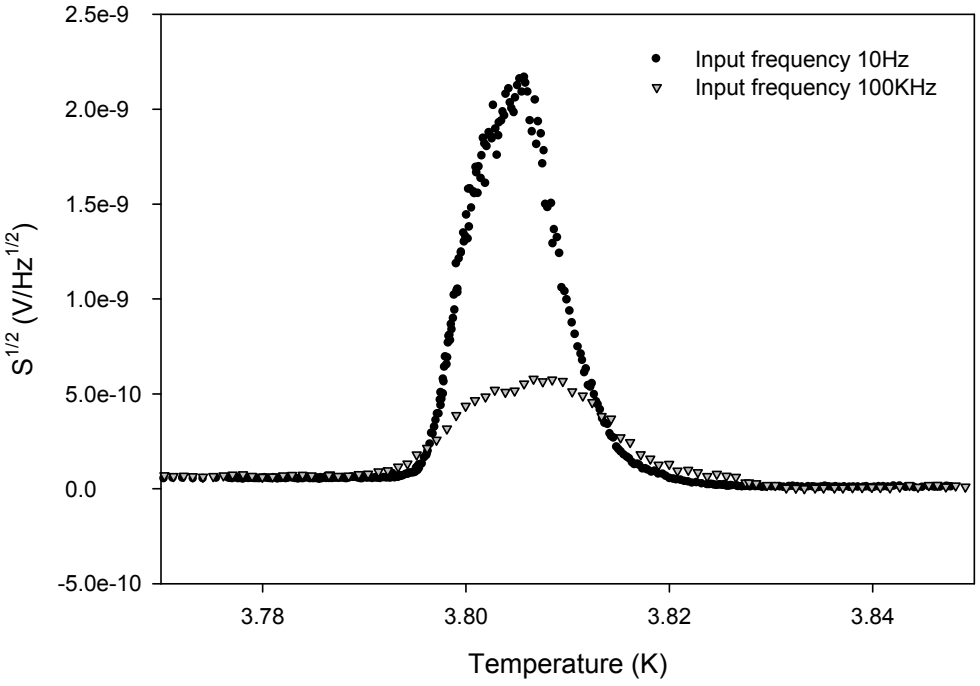

Fig 3.19 The temperature dependence of $S^{1/2}$ at different Freqency (Sample 4)

Since the fluctuation of the vortex pair separation process is the main source of the voltage noise with ac current, the voltage noise with ac current is suppose to be related with the frequency of excitation current. Shown in Fig 3.19 is the temperature dependence of the voltage noise density at different input frequency at 50μA. At 100 kHz, the voltage noise density is reduced considerably. However, no appreciable changes were

detected when the frequency of applied current is changed in either low or high limits.

3.4 I-V Characteristics and Excess Noises

The large excess noises observed in Tin films when alternating currents were applied suggest the vortex pair separation process plays an important role in the noise generation in the two dimensional superconducting transition. When an alternating current is applied, the perturbation to the reversible process of vortex pair separation is supposed to be strongly related with the amplitude of excitation current. To test the current dependence of the voltage noise density carefully, we have carried out simultaneous measurements of the current dependence of voltages and voltage noise density at fixed temperatures. The I-V characteristics of sample which we discussed in chapter 2 show that the term BI^3 in equation (2.4) describes the separation process of vortex pairs. If excess noises with alternating currents are mainly produced by the fluctuation of vortex pair separation process, the excess noises should be strongly related with the term BI^3.

Shown in Fig 3.20 is the relationship between I-V characteristics of sample and voltage noise density at 3.777K. The top graph in Fig 3.20 shows the current dependences of the fundamental voltage, the third harmonic voltage and the fifth harmonic voltage. The power index at this temperature is about 2 so that the log-log plot of fundamental voltage versus current includes two parts, linear term at small current and power term at big current. The plot of third harmonic voltage versus current is mainly decided by the

term BI^3 at this temperature and the slope of log-log plot of current-third harmonic voltage is three. The plot of current-third harmonic voltage describes the vortex pair separation process.

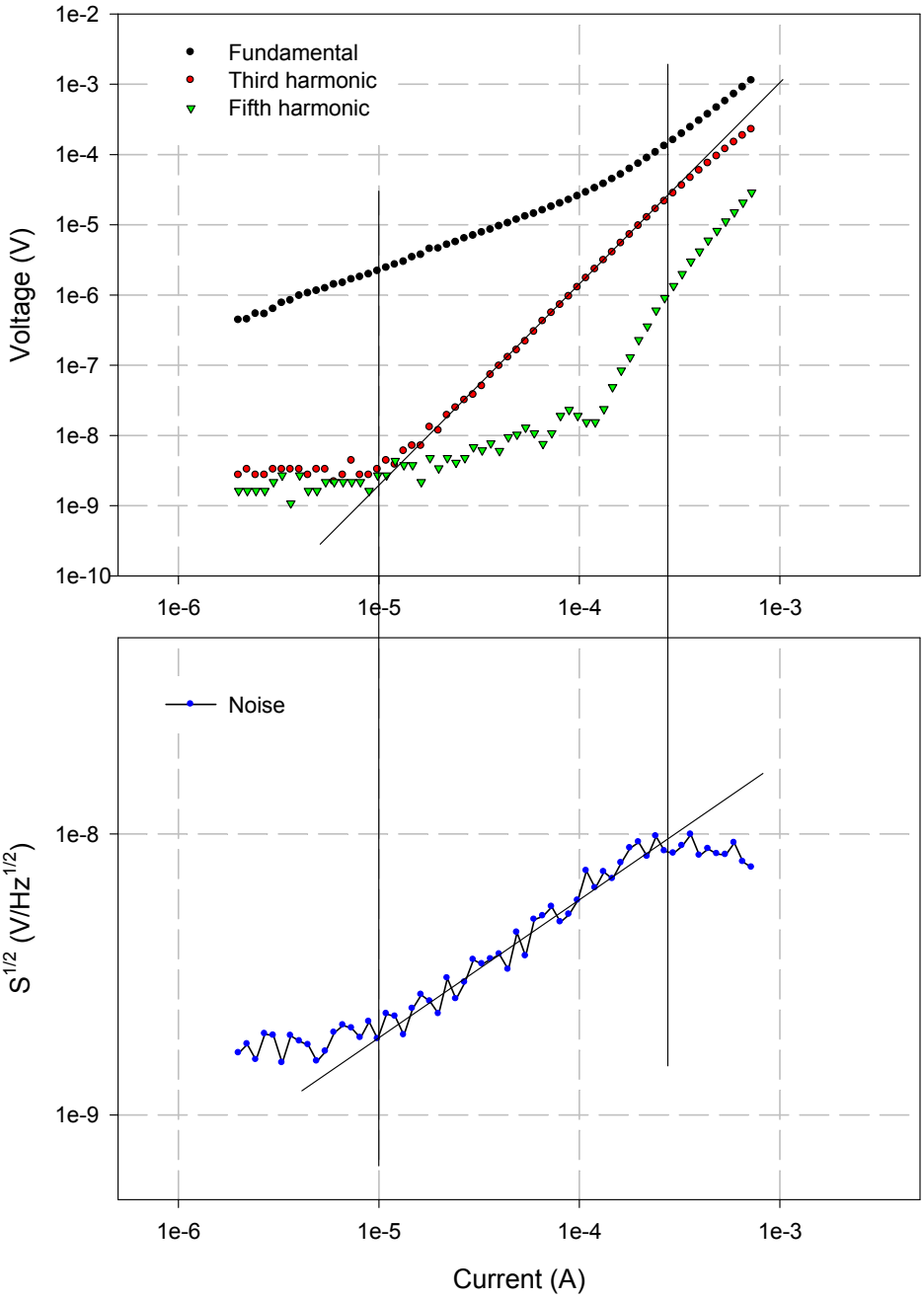

Fig 3.20 Current dependence of V and $S^{1/2}$ at 3.777K (Sample 11)

The bottom graph in Fig 3.20 shows the current dependence of voltage noise density. As can be seen from the graph, for small currents the third harmonic voltage is

not measurable, the noise is mainly attributed to the thermal perturbation and is almost independent on the amplitude of applied current. With the increasing current, the vortex pairs start to be separated by the applied current, so the third harmonic voltage appears and increases. The excess noise starts to increase at the same time with the third harmonic voltage appearing, and increases with the increasing third harmonic voltage. Until the power index of the log-log plot of current-third harmonic voltage does not keep three any more at big current, the excess noise does not increase any more either. This I-V characteristic at big current is attributed to the interaction of vortices, which is increased with the increasing current and will depress the fluctuation at big current. This synchronization of the excess noise and the third harmonic voltage suggests that the fluctuation of vortex pair separation process is one of the sources of excess noise in two dimensional samples and sometimes dominated the generation of excess noise when alternating currents are applied.

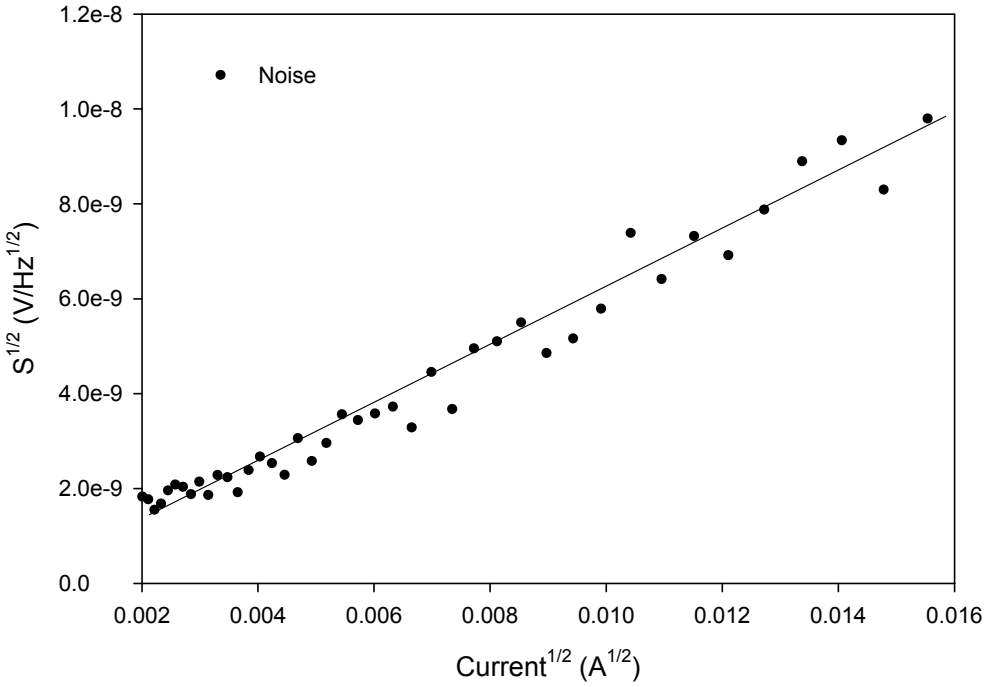

Fig 3.21 The linear dependence of $S^{1/2}$ versus $I^{1/2}$ at 3.777K (Sample 11)

Since the excess noise is dominated by the fluctuation of vortex pair separation process in a range of current, the excess noise is suppose to be strongly related with the amplitude of excitation current which is related with the perturbation amplitude. The bottom graph in Fig 3.20 shows that the slope of the log-log plot of voltage noise density versus current for the intermediate current is about 1/2, which means the voltage noise density is linear with the square root of current. Shown in Fig 3.21 is the linear dependence of voltage noise density as a function of the square root of current.

Shown in Fig 3.22 is the linear dependence of voltage noise density as a function of the square root of voltage at 3.777K. This linear dependence is qualitatively consistent with the nature of shot noise, i.e., the noise produced by the fluctuation of vortex pair separation process is shot noise at small applied current.

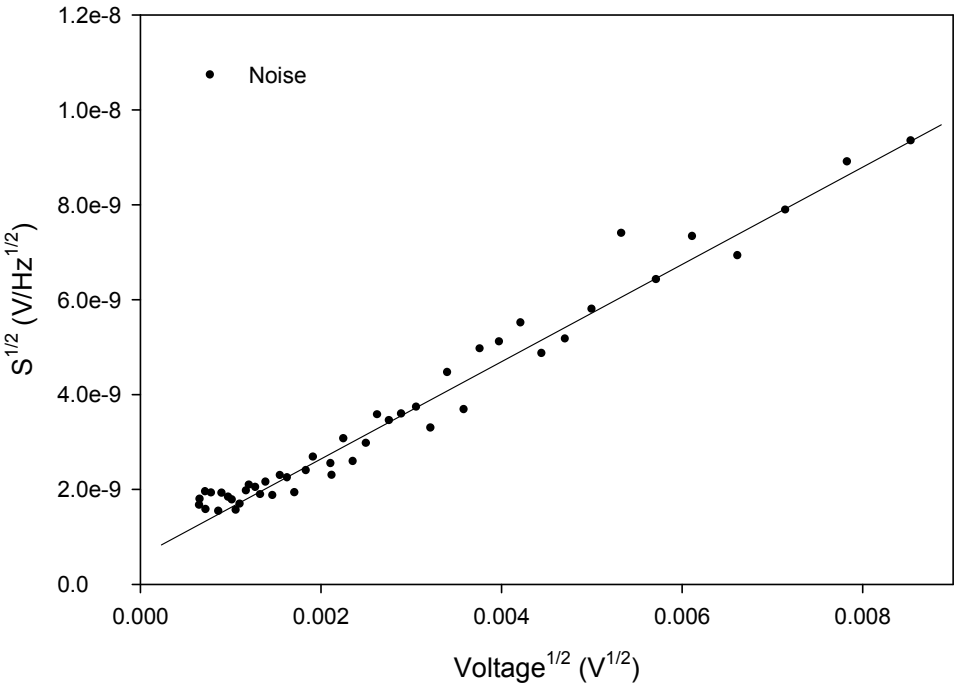

Fig 3.22 The linear dependence of $S^{1/2}$ versus $V^{1/2}$ at 3.777K (Sample 11)

Early work about the shot noises in Tin films with direct currents have been reported and discussed [41,42]. The samples studied earlier were generally 100-1000

times more resistive than our samples, but the superconducting transitions appear very similar. The similar linear dependence of $S^{1/2}$ in $V^{1/2}$ was observed and attributed to the phase-slip shot noise due to independent vortex motion across the width of sample. The noise power of phase shot noise was given by

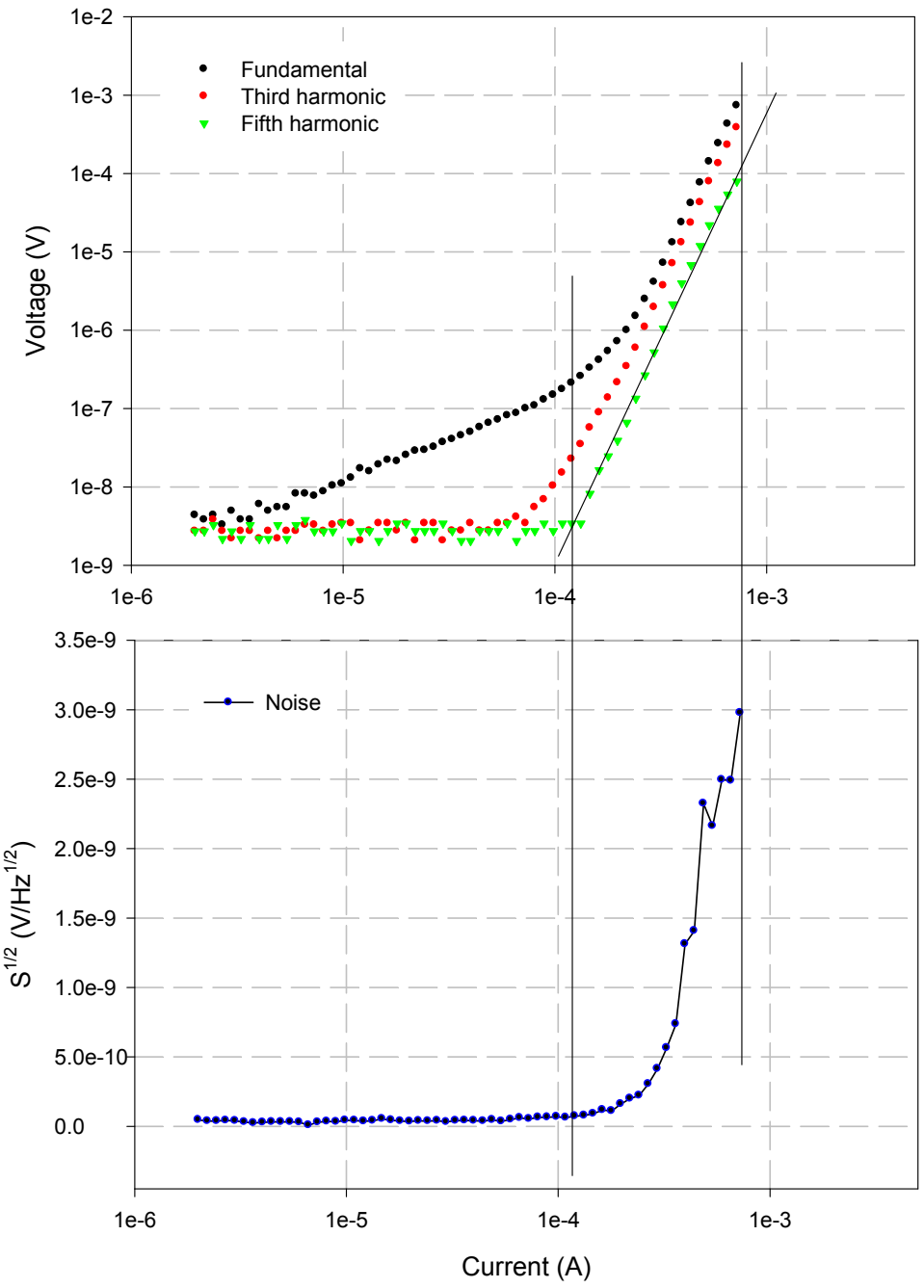

Fig 3.23 Current dependence of V and $S^{1/2}$ at 3.767K (Sample 11)

$$S = 2\frac{\varphi_0 \Delta\varphi}{2\pi} V_{dc}$$

Thus the largest slope of the simple shot noise is $\sqrt{2\varphi_0} = 0.6\times10^{-7}$. However the magnitude of slope derived from our experimental results vary from $(1-10)\times10^{-7}$ which suggested the excess noise produced by the fluctuation of vortex pair separation process in alternating excitation current is much bigger than the phase-slip shot noise due to the independent vortex motion in dc.

When the temperature decreased and the power index of I-V characteristic at this temperature is bigger than 5, the third harmonic voltage and the fifth harmonic voltage would be determined by the item CI^5 in equation (2.4) which is attributed to the vortex pair-pairs in samples. Our results show the noise with ac current at this temperature will be determined by the term CI^5.

Shown in Fig 3.23 is the relationship between the I-V characteristics of sample and the voltage noise density at 3.767K. The top graph shows the current dependences of the fundamental voltage, the third harmonic voltage and the fifth harmonic voltage. The bottom graph shows the current dependence of voltage noise density. According to the graphs, the voltage noise density starts at the same time with the appearance of the fifth harmonic voltage. But different with Fig 3.20, the voltage noise density does not linearly increase with the square root of current, instead of increases very fast with the increasing current. But similar to the result above, there is still linear dependence of voltage noise density as a function of the square root of voltage at this temperature, which suggests the excess noise attributed to the vortex pair-pairs in alternating excitation current is shot noise too. Shown in Fig 3.24 is the linear dependence of voltage noise density as a

function of the square root of voltage at 3.767K.

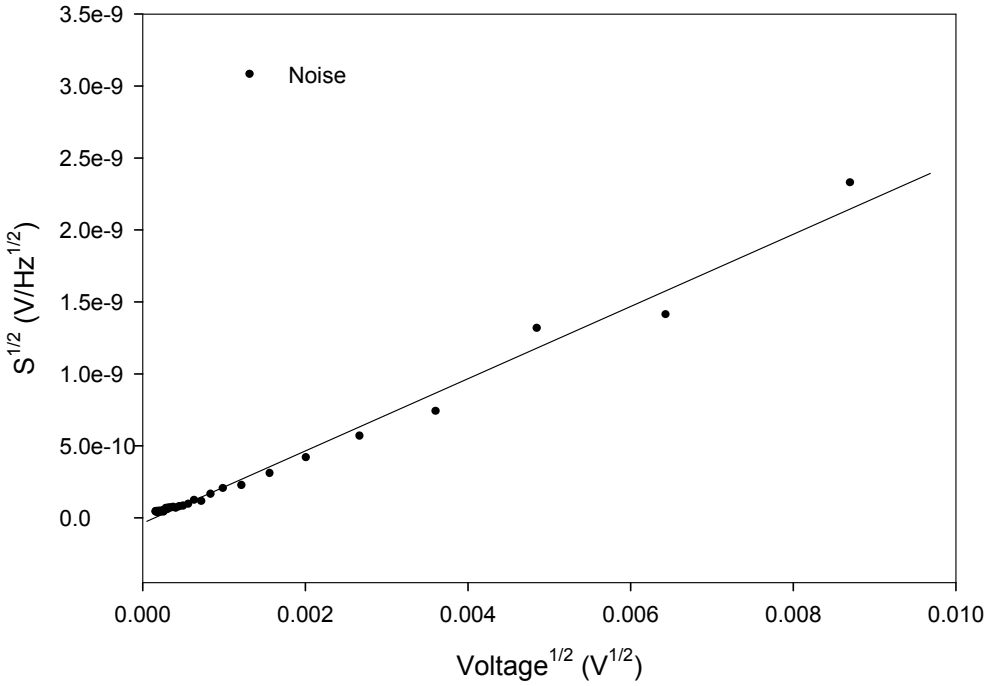

Fig 3.24 The linear dependence of $S^{1/2}$ versus $V^{1/2}$ at 3.767K (Sample 11)

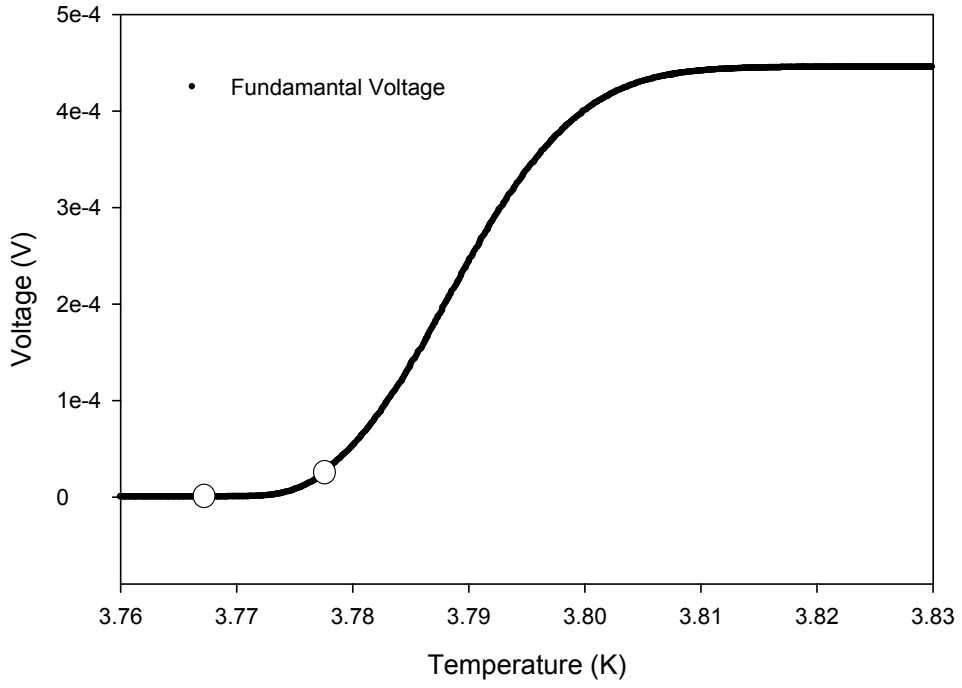

Fig 3.25 The temperature dependence of the fundamental voltage (Sample 11)

Since the higher power terms only exist at a small range of temperature width in superconducting transition, the excess noises with ac in the entire transition are supposed

to be mainly determined by the term BI^3, i.e., determined by the separation process of vortex pairs. Shown in Fig 3.25 is the temperature dependence of the fundamental voltage at 100μA. The two circles in Fig 3.25 indicate the temperatures of last two cases we just discussed above. Both of them are at the lower temperature side of superconducting transition. For the most part of transition process, the relationship between the I-V characteristic and the excess noise is supposed to be similar to the case at 3.777K, i.e., the excess noise will be strongly related with the third harmonic voltage.

If the applied current is not very big where the interaction of vortices is not very big, the electrical response of sample will be dominated by the vortex pair separation process for most part of transition process, the temperature dependence of excess noise is suppose to be strongly related with the temperature dependence of the third harmonic voltage. According to Fig 3.18, the peak of voltage noise density of sample 14 at 200μA is mainly dominated by the fluctuation of the vortex pair separation process, so the similar temperature dependences of the third harmonic voltage and the excess noise in the entire transition process are expected at 200μA. Shown in Fig 3.26 is an overlay of the temperature dependence of the voltage noise density $s^{1/2}$ and the third harmonic voltage when 200μA alternating current is applied. The voltage noise density is multiplied by 8.33×10^{-8} to be displayed on the same scale as the third harmonic voltage. The coincidence of these two plots in Fig 3.26 shows the excess noise with ac is mainly produced by the fluctuation of the vortex pair separation process in most range of transition process at 200μA. The result in Fig 3.26 provides further evidence to support the model discussed in this thesis.

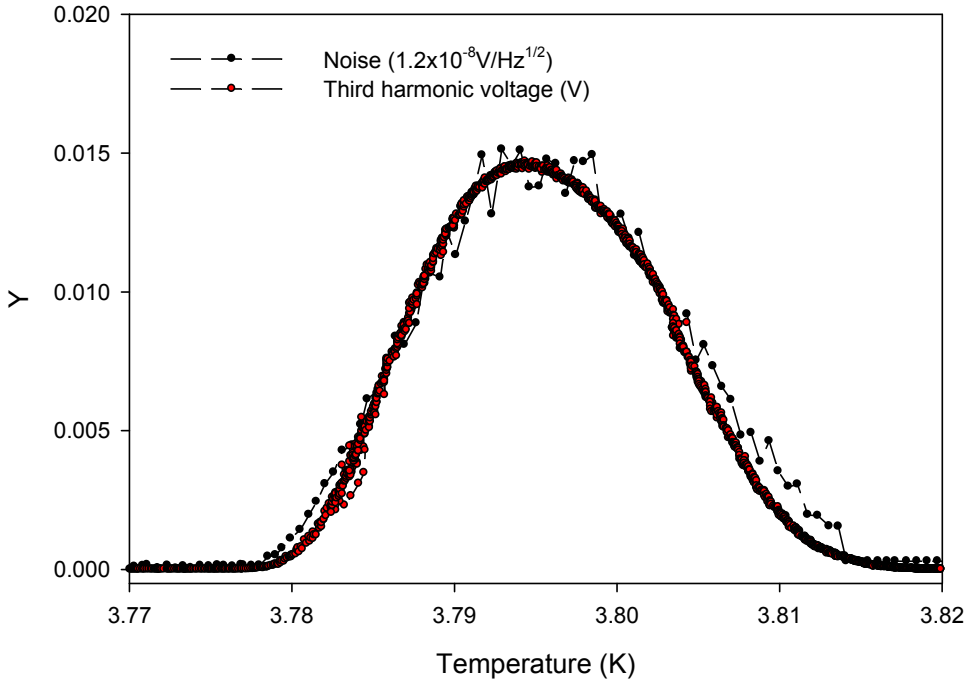

Fig 3.26 The temperature dependence of the $S^{1/2}$ and V (Sample 14)

Chapter 4 Conclusion

In this dissertation, the I-V characteristics and the excess noises of Tin films in the superconducting transition are studied. I-V characteristic measurement is a very important method to study the flux motion, vortex pinning mechanism and dimensional crossover in superconducting transition. Normally the I-V characteristics in the two dimensional superconducting transition associated with direct currents are given by

$$V = KI^{\alpha}$$

We found this equation is not satisfied when a sine wave alternating current is applied as the excitation current. To describe the I-V characteristics of two dimensional samples with alternating applied currents, a new equation is suggested according to the experimental results

$$V = AI + BI^3 + CI^5 + DI^7 + \cdots$$

where coefficient A, B, C and D depend on the temperature of sample. The first term AI is attributed to the free vortex motion and the coefficient A should be linear with the resistance of sample. Because the interaction of two vortices is linear with $(I\phi)^2$, the second term BI^3 is supposed to be the contribution of the separation of vortex pairs. Same as the analysis above, the third term CI^5 can be considered the contribution of vortex pair-pairs.

The equation above is supported by the experimental results. In this work the fundamental voltage, the third harmonic voltage and the fifth harmonic voltage are measured at the same time by the SR760 spectrum analyzer. The plots of the applied

current versus the voltages and the ratios of different harmonic voltages prove that the equation above can describe the electric response of Tin films with ac currents. At low temperatures, only high power index terms are present in the I-V curves. With the increasing temperature, the term CI^5 appears and vortex pair-pairs dominate the electric response of sample. Then vortex pairs are produced in sample with the increasing temperature and dominate the electric response of Tin films.

The free vortices will start to be produced by thermal energy when the temperature reaches the critical temperature of K-T transition, thus the linear relationship will appear in the plot of the current-fundamental voltage characteristic of sample. The slope of log-log plot of current-fundamental voltage for big current will be less than three, and will decrease with the increasing free vortices in sample which are produced with the increasing temperature.

The current-voltage characteristics of Tin films with ac current can help us to understand the vortex motion in the superconducting transition in two dimensional samples. The plots of the current-fundamental voltage characteristic of sample can help us to understand the K-T transition and figure out the critical temperature of K-T transition. The plots of the current-third harmonic voltage characteristic of sample can help us to figure out the critical temperature at which the vortex pairs start to be separated by the applied current. At last, the relationship of the current-voltage characteristics and the excess noises with ac can help us to understand the source of excess noises of two dimensional samples.

In this work voltage noises were measured as a function of temperature and dc or ac

current. The voltage noise density depends strongly on the temperature and current. Since the excess noise is related with the motion of free vortices in samples, the excess noise is supposed to depend on the number of free vortices which is related to the resistance of sample. The relationship of excess noise and resistance of sample in ac is carefully studied and an empirical function of voltage noise density in term of resistance for the entire transition is given by

$$S^{1/2} = \begin{cases} AR & R < 3\%R_0 \\ B\log(R) & 3\%R_0 < R < \frac{3}{7}R_0, \ \textit{before the peak} \\ CR & R > \frac{3}{7}R_0, \ \textit{after the peak} \end{cases}$$

where R_0 is the resistance of sample in normal state. This empirical function is satisfied with different applied alternating currents. Both the voltage noise density and the derivative of resistance are strongly peaked during the transition, but the peak of voltage noise density is a slightly shifted toward the lower temperature from the peak of the derivative of resistance.

Since there is a reversible process of vortex pair separation in two dimensional samples in superconducting transition, the number of vortex pairs and free vortices will fluctuate with the applied alternating current. Different from the direct applied current, the noises of Tin films with ac will be dominated by the fluctuation of the vortex pair separation process, which is much bigger than the fluctuation produced by the thermal perturbation in dc. Our experimental results show that the excess noise with ac current is much bigger than the excess noise with dc current, sometimes as big as ten times of that of dc at the same amplitude of current.

Because the excess noise with alternating applied current is dominated by the fluctuation of the vortex pair separation process, the excess noise with ac should be strongly related with the amplitude of excitation current. Experimental results show that the peak of voltage noise density is linear with the amplitude of excitation current until the current is big enough that the interaction of vortices will depress the fluctuation of vortex pair separation process. Experimental results also show that the voltage noise density with ac current is more sensitive to the excitation current variations than the excess noise with dc current for most range of current.

At the lower temperature side of superconducting transition, the number of free vortices produced by thermal perturbation is small and the electrical response of sample is dominated by the vortex pairs. The fluctuation of the number of free vortices can be neglected and there is no excess noise with direct current at this temperature. However, appreciable vortex noise due to the fluctuation of vortex pair separation process can be measured at this temperature when an alternating current is applied. So the excess noise with alternating current will appear first with the increasing temperature, and the excess noise with dc current will appear at a higher temperature than that of ac current as demonstrated in experimental results.

The excess noise with ac current is dominated by the fluctuation of the vortex pair separation process in Tin films, thus the excess noise is supposed to be strongly related with the amplitude of excitation current. To examine the current dependence of the voltage noise density carefully, we have carried out simultaneous measurement of the current dependence of voltages and voltage noise density at fixed temperatures.

Experimental results show that for the most temperature of transition width, the excess noises start to appear with the increasing current at the same time as the appearance of the third harmonic voltage. We know that the third harmonic voltage is mainly attributed to the vortex pair separation process, this coincidence is a solid proof that the excess noise with ac current is dominated by the fluctuation of the vortex pair separation process. The voltage noise density under this condition is linear with the square root of current. The voltage noise density in small voltage is linear with the square root of applied voltage which suggests the excess noise produced by the fluctuation of vortex pair separation process is shot noise. At lower temperatures, the electric response of sample is dominated by the vortex pair-pairs. The excess noises start to appear with the increasing current at the same time as the appearance of the fifth harmonic voltage. The voltage noise density at this temperatures increases much faster than the linear dependence of the square root of current. However, the voltage noise density still linear with the square root of applied voltage.

Furthermore, the temperature dependence of the third harmonic voltage and the voltage noise density in entire transition are measured. Since the higher power terms only exist at a small range of temperature width in the superconducting transition, the excess noise with ac current in the entire transition is supposed to be mainly determined by the term BI^3, i.e., determined by the fluctuation of the vortex pair separation process. The temperature dependence of excess noise is expected to be strongly related with the temperature dependence of the third harmonic voltage. Our experimental results show that the temperature dependence of voltage noise density is almost identical with that of

the third harmonic voltage. The result suggests strongly that the excess noise with ac current is dominated by the fluctuation of the vortex pair separation process.

According to the discussion above, the excess noises in the superconducting transition in two dimensional samples, including the excess noises in the transition edge sensors, are not only produced by the thermal perturbation, but also produced by the fluctuation of vortex pair separation process. Our experiments using the alternating current to be the excitation current have revealed very rich structures in the current-voltage relationship and increased significantly the excess noise in superconducting transition. The comparison of the excess noise between with ac current and with dc current and the relationship between the I-V characteristics and the excess noises provide strong evidence that the fluctuation of vortex pair separation process is an important source of excess noises in the two dimensional superconducting transition.

Since there is a reversible process of vortex pair separation in the two dimensional superconducting transition, a small alternating signal will produce a big excess noise in two dimensional samples. Care should be taken to minimize the ac pickup. Thus to decrease the excess noise in superconducting transition, it is important to shield the samples and the instruments to block out external electrical fields. It is also very important to decrease the fluctuation of current and to avoid any alternating signal induction in two dimensional samples.

References

[1] H. Kamerlingh Onners, Leiden Comm. 120b, 122b, 124c (1911)

[2] W. Meissner and R. Ochsenfeld, Naturwissenschaften 21, 787(1933)

[3] F. London, Superfluids, Vol. I, Wiley, New York, 1950

[4] A. A. Abrikosov, Sov Phys. JETP 5, 1174(1957)

[5] A. Moser et al., Phys. Rev. Lett. 74, 1847 (1995)

[6] U. Essmann and H. Trauble, Phys. Letters 24A, 526(1967)

[7] P. L. Gammel et al., Phys. Rev. Lett. 59, 2592 (1987)

[8] G. J. Dolan et al., Phys. Rev. Lett. 62, 827 (1989)

[9] H. F. Hess et al., Phys. Rev. Lett. 62, 214 (1989)

[10] J. E. Bonevich et al,. Phys. Rev. Lett. 70, 2952 (1993)

[11] D. J. van Ooijen and G. J. van Gurp, Phys. Letters 17, 230(1965)

[12] P. W. Anderson, Phys. Rev. Letters 9, 309 (1962)

[13] P. W. Anderson and Y. B. Kim, Rev. Mod. Phys. 36, 39 (1964)

[14] M. Tinkham, Phys. Rev. Lett. 13, 804 (1964)

[15] C. Dekker et al., Phys. Rev. Lett. 69, 2717 (1992)

[16] Bairu Zhao et al., Phys. Rev. B 55, 1247 (1997)

[17] M. P. A. Fisher, Phys. Rev. Lett. 62, 1415 (1989)

[18] D. S. Fisher, Phys. Rev. B 43, 130 (1991)

[19] J. M. Kosterlitz and D. J. Thouless, J. Phys. C 6, 1181 (1973)

[20] V. L. Berezinskii, Sov. Phys. JETP 32, 493 (1970)

[21] M. Ban et al., Phys. Rev. B 40, 4419 (1989)

[22] Y. Ando et al., Phys. Rev. Lett., 67, 2737 (1991)

[23] C. T. Rogers et al., Phys. Rev. Lett., 69, 160 (1992)

[24] B. I. Halperin et al., J. Low Temp. Phys. 36, 599 (1979)

[25] A. F. Hebard et al., Phys. Rev. Lett. 50, 1603 (1983)

[26] E. Silver et al., X-ray and Gamma-ray Astronomy with NTD Germanium-based Microcalorimeters, AIP Conference Proceedings, 605, 555 (2001)

[27] K. D. Irwin et al., A Mo-Cu Superconducting Transition-Edge Microcalorimeter with 4.5ev Energy Resolution at 6Kev, Low Temperature Detectors 8, Nucl. Instr. and Meth. A, 444, 184 (2000)

[28] M. Galeazzi et al., Microcalorimeter and Bolometer Model, JAP 93, 4856

[29] J. C. Mather, Bolometer Noise: Nonequilibriu Theory, Appl. Opt. 21, 1225 (1982)

[30] M. A. Lindeman et al., TES Physics: Probing the Phase Transition, Talk given at the 1st International Workshop on TES, April, 2002

[31] W. Bergman-Tiest et al., Performance of X-ray Microcalorimeters with an Energy Resolution below 4.5eV and 100us response time, AIP Conference Proceedings, 605, 199 (2001)

[32] M. A. Lindeman et al., Performance of Mo/Au TES Microcalorimeters, AIP Conference Proceedings, 605, 203 (2001)

[33] P. Tan et al., Mo-Cu Bilayers as Transition Edge Sensors for X-ray Astrophysics, AIP Conference Proceedings, 605, 255 (2001)

[34] R. P. Huebener et al., Current-Induced Intermediate State in Thin-Film Type-I Superconductors: Electrical Resistance and Noise, Phys. Rev. B, 7, 4089 (1973)

[35] P. R. Solomon, Flux Motion in Type-I Superconductors, Phys. Rev. 179, 475 (1969)

[36] P. M. Horn et al., Flux Flow and Fluctuation Effects in Granular Superconducting Films, Phys. Rev. B, 4, 2178 (1971)

[37] P. R. Solomon et al., Current-Induced Flow of Domains in the Intermediate State of a Superconductor, Phys. Rev. B, 3, 2969 (1971)

[38] R. Ikeda et al., Theory of Broad Resistive Transition in High Temperature Superconductors under Magnetic Field, J Phys. Soc. Jpn. 60(3), 1051 (1990)

[39] A. A. Varlamov et al., The Role of Density of States Fluctuations in the Normal State Properties of High T_C Superconductors, Advances in Physics 48(6), 655 (1999)

[40] C. M. Knoedler et al., J. Appl. Phys. 54 2773 (1983)

[41] R. F. Voss et al., Phys. Rev. Lett. 45, 1523 (1980)

[42] C. M. Knoedler and Richard F. Voss, Phys. Rev. B 26, 449 (1982)